Volume 5, Issue 2, December 2019 ISSN 2356-8569

ACADEMY Publishing Center

Journal of Renewable Energy and Sustainable Development

RESD

Academy Publishing Center
Journal of Renewable Energy and Sustainable Development (RESD)
First edition 2015

Permissions may be sought directly Academy Publishing Center,
Arab Academy for Science, Technology, and Maritime Transport, AASTMT
Abu Kir Campus, Alexandria, EGYPT
P.O. Box: Miami 1029
Tel: (+203) 5622366/88 – EXT 1069 and (+203) 5611818
Fax: (+203) 5611818
Web Site: http://apc.aast.edu

Volume 5, Issue 2, December 2019

ISSN: 2356-8518 Print Version

ISSN: 2356-8569 Online Version

RESD

Journal of Renewable Energy and Sustainable Development

Renewable Energy and Sustainable Development (RESD) is a biannual international peer-reviewed journal, which presents a global forum for dissemination of research articles, case studies and reviews focusing on all aspects of renewable energy and its role in sustainable development. The topics of focal interest to RESD include, but are not limited to, all aspects of wind energy, wave/tidal energy, solar energy, as well as energy from biomass and biofuel. The integration of renewable energy technologies in electrical power networks and smart grids is another topic of interest to RESD. Experimental, computational and theoretical studies are all welcomed to RESD.

Sustainable development is a multidisciplinary advancing to the center of energy research with the declaration of UN millennium development goals for the first time in 2000, and continued to constitute a challenge in energy technologies in the past decade. RESD is mainly interested in case studies of sustainable development and its relation to transition economies in the Middle East, Africa, Asia and Oceania.

RESD has an outstanding editorial board of eminent scientists, researchers and engineers who contribute and enrich the journal with their vast experience in different fields of interest to the journal. The journal is open-access with a liberal Creative Commons Attribution-Non Commercial-4.0 International License. Which preserves the copyrights of published materials to the authors and protects it from unauthorized commercial use or derivation. The journal is financially supported by Arab Academy for Science, Technology and Maritime Transporting in order to maintain quality open-access source of research papers on renewable energy and sustainable development.

Editorial Committee

Peer Review Process

Peer review is an objective process at the heart of good scholarly publishing and is carried out on all reputable scientific journals. Our referees therefore play a vital role in maintaining the high standards of Renewable Energy and Sustainable Development (RESD) and all manuscripts are peer reviewed following the procedure outlined below.

Overall process for publishing a paper will be taken approximately 4 months after initial submission. Reviewing process will take about 2 months, and then publishing process will not exceed 2 months.

1. Initial manuscript evaluation

The Editor first evaluates all manuscripts. It is rare, but it is entirely feasible for an exceptional manuscript to be accepted at this stage. Those rejected at this stage are insufficiently original, have serious scientific flaws, have poor grammar or English language, or are outside the aims and scope of the journal. Those that meet the minimum criteria are passed on to at least 2 experts for review.

Authors of manuscripts rejected at this stage will normally be informed within 2 to 3 weeks of receipt.

2. Type of Peer Review

This journal employs single blind reviewing, the author identity is disclosed to the referee, while the referee remains anonymous throughout the process.

3. How the referee is selected

Referees are matched to the paper according to their expertise. Our database is constantly being updated. RESD has a policy of using single blind refereeing (as detailed in the previous section), with neither referee from the country of the submitting author. We welcome suggestions for referees from the author though these recommendations may or may not be used.

4. Referee reports

Referees are asked to evaluate whether the manuscript support followings key points related to scientific content, quality and presentation:

4.1. Technical

Scientific merit: notably scientific rigour, accuracy and correctness.

Clarity of expression; communication of ideas; readability and discussion of concepts. Sufficient

discussion of the context of the work, and suitable referencing.

4.2. Quality

Originality: Is the work relevant and novel?

Motivation: Does the problem considered have a sound motivation? All papers should clearly demonstrate the scientific interest of the results.

Repetition: Have significant parts of the manuscript already been published? Length: Is the

content of the work of sufficient scientific interest to justify its length?

4.3. Presentation

Title: Is it adequate and appropriate for the content of the article?

Abstract: Does it contain the essential information of the article? Is it complete? Is it suitable for inclusion by itself in an abstracting service?

Diagrams, figures, tables and captions: Are they essential and clear?

Text and mathematics: Are they brief but still clear? If you recommend shortening, please suggest what should be omitted.

Conclusion: Does the paper contain a carefully written conclusion, summarizing what has been learned and why it is interesting and useful?

Referees are not expected to correct or copyedit manuscripts. Language correction is not part of the peer review process.

5. How long does the review process take?

Typically the manuscript will be reviewed within 3 months. Should the referees' reports contradict one another or a report is unnecessarily delayed a further expert opinion will be sought. All our referees sign a conflict of interest statement. Revised manuscripts are usually returned to the initial referees within 1 week. Referees may request more than one revision of a manuscript.

6. Editorial decisions

After peer review and referee recommendation, the editor-in-chief, with the assistance of the associate editor, will study the paper together with reviewer comments to make one of the following decisions.

Accept

Accept pending minor revision: no external review required Reject/Resubmit: major

revisions needed and a new peer-review required Reject

Digital Object Identifier

The RESD is supported by Digital Object Identifier, DOI for each article from Cross Ref.

The Code of the DOI of each article consists of the following format:

10.21622/RESD.YYYY.VV.I.PPP Where

10.21622	= Journal Identifier
RESD	= Journal name
YYYY	= Four digits for the year
VV	= Two digits for the Volume Number
I	= One digit for the Issue Number
PPP	= Three digits for the Number of the first page of the article

To look for the paper on line, search for this link
http://dx.doi.org/10.21622/RESD.YYYY.VV.I.PPP

Table of Contents

Editorials

Articles

Journal of Renewable Energy and Sustainable Development (RESD) Volume 5, Issue 2, December 2019 - ISSN 2356-8569
http://dx.doi.org/10.21622/RESD.2019.05.2.044

Renewable Energy Sources and the New Paradigm in Energy Engineering

Prof. Eden MAMUT, Director
Institute for Nanotechnologies & Alternative Energy Sources
"Ovidius" University of Constanta, Romania
Email: eden.mamut@et-is.eu

After centuries of scientific, industrial and technological achievements the current paradigm in energy engineering may be defined as the complex set of knowledge, technologies, policies but even individual and community attitudes aiming to assure at the level of each energy end-user the required quantity and quality of energy, at minimum price and with minimal impact on the environment on a life cycle reasoning from production to final use.

In 2012, I had the chance to participate at the UN Conference on Sustainable Development organized at Rio de Janeiro, the so called "Rio + 20" Conference, as a member of the Official Delegation of Romania and at the same time representing the UN Academic Impact Initiative. On that position, I had the possibility to join many sessions of the Conference and to follow also the process of negotiations for the text of the Final Declaration of the Conference. Passing from one session to another, there were several aspects that were confusing me.

One of them was a declaration of the representative of a large company from Brazil, mentioning that his country has a huge stockpile of biomass and if it shall be used as bioenergy resource, it is plenty to assure the welfare of that country. The confusion for me was if a Global Ecosystem as the Amazonian Forest, could be considered an asset to be exploited at the discretion of some local groups of interest. It is well known, that the complexity of the factors that are interlinked with the biomass in different ecosystems it is not yet very clear even for small ecosystems. The current attempts to develop detailed Multiscale and Multiphysics models for parts of the deltas of Mississippi River in the US or Danube Delta in Europe are in some initial stages and there will be needed decades of scientific research for developing comprehensive models for global macro-ecosystems like the Nile or the Amazonian.

Unfortunately, at present, the quotas for exploiting resources as forest wood or reed in wetlands or Deltas in many parts of the World are established without any scientific background. But many published reports reveled that even the simple question: *"what is the percentage of straw that is yielded from a hectare of wheat that may be used for energy or industrial purpose?"* has the answer *"depends on many factors"*. With interdisciplinary and cross-disciplinary approaches, reliable tools and methods may be developed to strengthen the methodologies as *"ecosystem services"* and this movement has to be further multiplied in order to become a norm.

As an example, in the Black Sea Region we have developed an Alliance of Space research centers to aggregate satellite data with advanced computing codes in order to evaluate the potential of exploitation of renewable energy resources as biomass, solar, wind or water currents and similar initiatives are also in many other regions of the World. The most important aspect that we learn, is that renewable energy sources have no borders and even the very rudimental tools that we have yet, allow us to understand that there are situations when between a large storm in the Sahara desert and the yield of biomass from the Amazonian Delta may be many interlinked and influencing factors.

The major disappointment at the end of "Rio + 20" Conference held in 2012, was that the final resolution was blocked by the group of the Non-Aligned Countries on the argument that the developed countries have already a set of technologies on the shelf and would like to impose them to the developing countries. Such an argument is very often promoted in different Conferences or meetings organized at certain levels. As an example, in Romania, the scientific research activities on wind energy have started in 1974 as a National Program for Alternative Energy Sources. Over many decades, there were spent significant amounts of funds for developing original solutions and technologies. Unfortunately, the scientific research achievements have not been transferred to industry and business. As a consequence, when Romania joined the EU in 2007 and specific subsidy programs have been initiated to promote renewable energy sources, all investment projects on wind farms have been developed with technologies from the developed countries. It took us several years to understand the very important connection between the scientific research, innovation and competitiveness at regional and global scales.

http://dx.doi.org/10.21622/RESD.2019.05.2.044

At present, at the Institute for Nanotechnologies and Alternative Energy Sources, at "Ovidius" University of Constanta, we have established a special framework for cooperation between Academia and Industry. We are working together with 9 companies on developing competitive products and services integrating nanomaterials and nanotechnologies. The solutions that are developed by joint team of researchers from our institute and partner companies include antistatic paints for solar PV and thermal panels for the reduction of dust depositions and securing their performances, anti-corrosion solutions for heat pump installations in coastal areas using sea water, catalytic filters for waste biomass boilers to facilitate the combustion of a wide range of waste biomass, nanofluid based oils for high performance ORC installations, hybrid solar panels, MEAs for urea fuel cells but also IoS and IoT solutions for monitoring and system control. Putting in the forefront the industry, we try to improve their competitiveness and to build trust in cooperation with other players within the EU and worldwide.

In 2015, in New York, the UN General Assembly adopted the 2030 Agenda for Sustainable Development and the Sustainable Development Goals (SDGs), which include a dedicated goal on energy, SDG 7, calling to *"ensure access to affordable, reliable, sustainable and modern energy for all"*. It is also important to mention the fact that Energy, lies at the heart of both the 2030 Agenda for Sustainable Development and the Paris Agreement on Climate Change.

A fundamental element to support the SDG 7, is to facilitate to all the citizens of the World the access to up-to-date knowledge which includes the Open Access to scientific research results. But, in a document of the European Commission [1] developed based on a comprehensive analysis of a large volume of scientific publications, it is mentioned that *"Mostly due to current methods of capture and data malpractice, approximately 50% of all research data and experiments is considered not reproducible, and the vast majority (likely over 80%) of data never makes it to a trusted and sustainable repository."* In this respect, the Open Science movement including the aspects related to Open Access to the content of Scientific Journals, the Openness of the entire cycle of the scientific research process and the FAIR principles to publish data and metadata, may be also considered as a basic attempt for addressing the implementation of SDG 7.

This year, the Black Sea Universities Network established a pilot project on Open Science dedicated to the risks and vulnerabilities of using manufactured nanomaterials involving a group of researchers and with the support of the European Nanosafety Cluster and this process shall be further extended.

In the new paradigm of energy engineering, the symbiotic link between energy and information led to a fundamentally new approach on energy modeling. Recently, we started a new project under EU H2020 with a very valuable Europe wide consortium dedicated to the integration of waste heat streams from the industry in the District Heating systems. The approach that we are developing is to use massive data sets captured from a large variety of sensors and to develop Big Data and various other dedicated data mining tools for understanding the consumption characteristics of end-users, the matching with the available waste heat streams from local industries and with local resources of renewable energy. As a consequence, in the new paradigm, the optimization solutions are shifting from compliance with simple objective functions (as minimal cost or minimal impact) towards compliance with complex, dynamic, data driven solutions.

Reference:

[1] Realising the European Open Science Cloud, EC DG Research & Innovation 2016 http://ec.europa.eu/research/openscience/pdf/realising_the_european_open_science_cloud_2016.pdf#view=fit&pagemode=none

About Professor Prof. Eden MAMUT

Eden MAMUT is a Professor of Engineering Thermodynamics and Advanced Energy Systems at "Ovidius" University of Constanta, Romania, Director of the Institute for Nanotechnologies, Alternative Energy Sources, and Secretary General of the Black Sea Universities Network.

His field of research include: Advanced Energy Solutions based on nanomaterials and nanotechnologies, Multi scale thermo-fluid modeling, Analysis and optimization of complex energy systems, Renewable Energy Sources, Sustainable Transport Systems, Multi Criteria & Multi Scale Methods on Sustainable Development.

Prof. Mamut is author and co-author of 95 papers, 12 books (as author or editor), 2 registered patents (Germany), 3 registered patents (Romania).

Journal of Renewable Energy and Sustainable Development (RESD) Volume 5, Issue 2, December 2019 - ISSN 2356-8569
http://dx.doi.org/10.21622/RESD.2019.05.2.046

Probabilistic Analysis of the Reliability Performance for Power Transformers in Egypt

[1] Ahmed El-Bassiouny, [2] Mohamed El-Shimy, [3] Rizk Hamouda
[1] Salah Shaaban consulting office, Cairo, Egypt,
[2] Electrical Power and Machines Department, Faulty of Engineering, Ain Shams University, Cairo, Egypt,
[3] Energy Engineering, Faulty of Engineering, Heliopolis University, Cairo, Egypt,
[1]mohamed_bekhet@eng.asu.edu.eg

***Abstract* -** From reliability, maintainability, and availability (RAM) points of view, the performance of power transformers has significant impacts on the performance of the entire power network. Their performance has also significant impacts on the power interruptions at various voltage levels and the consequent customer interruption costs. This paper l discusses the estimated remaining lifetime of power transformers in 500 kV, 220 kV, 132 kV and 66-33 kV subpopulations of the Egyptian grid in which the best fit probability distribution is used through MATLAB program as the input data is time between failures (TBFs). The best fit probability distribution is used in this case study which is Weibull distribution. Finally, availability of the transformers per different voltage populations is calculated. Different subassemblies (failures) are also subjected to the same process of determining TBFs and estimating remaining lifetime. The results are helpful in the manufacturing process of the transformers and enhancing the maintenance schedule.

***Keywords* -** Transformers, Weibull distribution, Remaining lifetime, Availability.

I. INTRODUCTION

This paper discusses the probabilistic analysis of the reliability performance for the transformers of different voltage populations of the Egyptian Power Grid so that failure rates are calculated. Based on this, the overall performance of the transformer shall be observed. All the analyses are performed under probabilistic approach. The probabilistic analysis accounts for the uncertainties in the input data. The best fits of statistical probability distributions are determined for each transformer and for each of its subassemblies in various voltages subpopulations.

Main Data, collected of the Egyptian power grid from [1]-[3], are the number of transformers, number of failures, and repair time for every voltage subpopulation which are 500 kV, 220 kV, 132 kV and 66-33 kV of the Egyptian power grid from the year 2002 till 2009. The statistical approach is performed by using MATLAB program. Different continuous probability distributions were compared in order to obtain the best fit distribution for this case study. The input data is time between failures (TBFs) and Weibull distribution is used as a main distribution in this paper because it is widely and commonly used in reliability and lifetime analysis [4, 5, 6].

Remaining life time of the transformers in different voltage subpopulations are estimated by using the probability distributions and the results from the distributions will also be compared. Using Weibull distribution usually requires a defined failure time which is the time from the start of operation till failure occurred. Since the study period is only 8 years from year 2002 till year 2009, therefore time between failures (TBFs) is used in this paper since the TBFs units are years.

II. PROBABILITY DISTRIBUTIONS

Probability distributions are a mathematical method used to measure and analyze random variables [7]. Reliability engineering provides the methods and tools used to estimate the life time of equipment or components without failure for a specific period of time [8]. Probability distributions are categorized into continuous probability distributions and discrete probability distributions [9]. The selection of the most suitable probability distribution depends on every case. In this paper, since data are positive numbers and continuous, the selected distributions are Weibull distribution, Normal distribution, Rayleigh distribution, Logistic distribution and Lognormal distribution. Table (1) gives a summary regarding the five selected distributions.

Table 1 Summary of Five Different Probability Distributions.

	Probability Distribution	Type	Characteristics
1	Normal (Gaussian)	Continuous	It is used in reliability $$f(t) = \frac{1}{\sqrt{2\pi\sigma}} e^{\frac{-1}{2}(\frac{t-\mu}{\sigma})^2}$$ Where μ is the mean σ is the standard deviation
2	Logistic	Continuous	It is used to describe growth, that is, the size of a population expressed as a function of a time variable $$f(t) = \frac{e^{\frac{\mu-x}{\alpha}}}{\alpha[1+e^{\frac{\mu-x}{\alpha}}]}$$ μ is the mean or location parameter α is scale parameter
3	Weibull	Continuous	Used in reliability $$f(t) = \frac{\beta}{\eta} * \left(\frac{t}{\eta}\right)^{\beta-1} * e^{-(\frac{t}{\eta})^{\beta}}$$ β is shape parameter η is scale parameter
4	Lognormal	Continuous	It is used in Life time modelling and very helpful in Reliability engineering $$f(t) = \frac{1}{\sqrt{2\pi} * \sigma'} e^{\frac{-1}{2}(\frac{t'-\mu'}{\sigma'})^2}$$ t' = ln(t) μ' is the mean of Log time to fail σ' is the standard deviation of log time to fail
5	Rayleigh	Continuous	$$f(t) = 2 * \alpha * \lambda^2 * t * e^{-(\lambda * t)^2} * (1 - e^{-(\lambda * t)^2})^{\alpha-1}$$ α shape parameter λ scale parameter

2. A. Data Analysis and Remaining Lifetime Estimate of the Transformer

A. TBFs calculations

TBFs calculations for different voltage subpopulations are performed. All calculations are per transformer per year per failure. Figure (1) shows the different TBFs values for every voltage subpopulation where TBFs decrease as time increases indicating an increase in the failure rate. In comparison between different voltage subpopulations, 132 kV population has the highest TBF among the different voltage populations followed by 500 kV then 66-33 kV and finally 220 kV. These differences in TBFs between different voltages populations due to the fact that every sub voltage population has its own collected data.

B. Best fit distribution TBFs

After calculating TBFs, the second step is to determine the best suitable distribution by making a comparison between 5 different continuous distributions which are: Weibull distribution, Normal distribution, Rayleigh distribution, Logistic distribution, and Lognormal distribution. After getting Statistical mean and standard deviation results from MATLAB program, a percentage (%) difference of the mean and Standard Deviation (STD) is made between arithmetic and statistical values.

Normal distribution is a flexible distribution that fits parameters according to given values where the distribution is always symmetrical around the mean and mean, median and mode are always the same results [4, 10]. Accordingly, the Normal distribution is used in comparison and in obtaining the deterministic values only not in the ranking of the best fit distribution.

Table 2 summarizes the findings and indicates the best fit probability distribution in this case study. From the comparison between the distributions, Weibull distribution is common for all voltages subpopulations. This concludes that Weibull distribution is suitable for this case study. The second common distribution used is Lognormal distribution followed by Logistic distribution.

As per [5], the years with zero values shall be omitted from the population regarding Weibull distribution and as for Rayleigh distribution, it is a special deviation of Weibull distribution [11, 12] thus population with zero values are omitted, too. Therefore, for fair comparison, the study period is shortened and the results were obtained on this fact.

Weibull distribution acts as the main probability distribution in this paper in estimating the remaining life time of transformer. However, the Weibull distribution is under the investigation as like the other 4 probability distributions. This does not mean that Weibull distribution is not used in lifetime calculation, but it could not be suitable for this case only, also Weibull distribution has proven a high efficiency in lifetime analysis [13, 14].

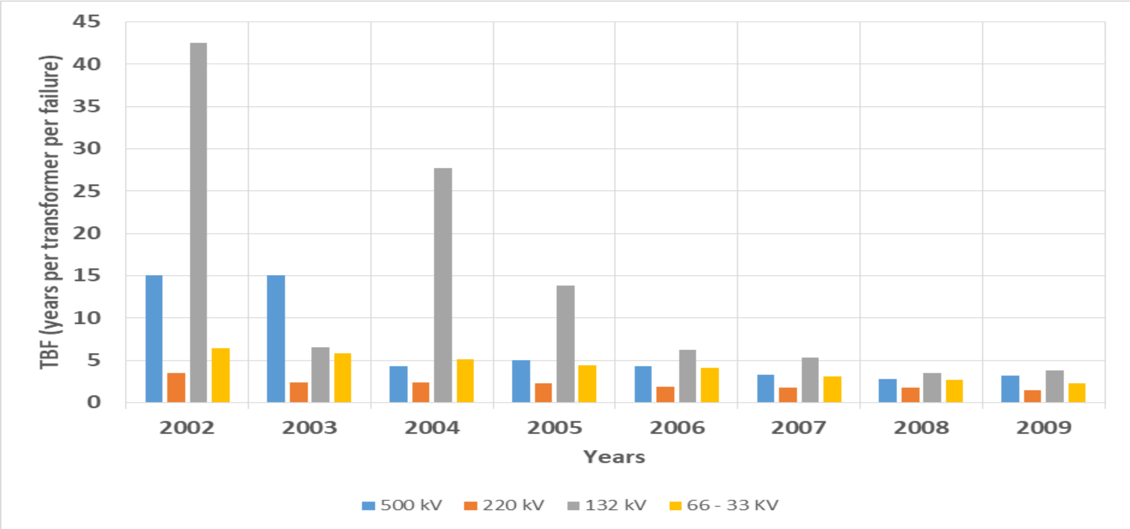

Fig .1 TBFs for different voltage populations

Table 2 Summary Table Indicating Best Fit Distributions for Every Voltage Subpopulation

Voltage Subpopulation	Probability Distribution used TBFs
500 kV	Lognormal & Weibull
220 kV	Weibull & Lognormal
132 kV	Weibull & Lognormal
66-33 kV	Weibull & Logistic

III. ESTIMATING THE REMAINING LIFETIME OF THE TRANSFORMERS

The study period is 8 years from the year 2002 to year 2009 and by using probability distributions as in table 2, TBFs will be the main input to the distributions in order to predict the remaining lifetime of the transformers. MATLAB program is used in the analysis where distribution fitter application in MATLAB is a very useful tool for the analysis. As for Weibull distribution, parameters estimation in MATLAB coding is by the method of Maximum Likelihood Estimation [15, 16] where this method is the most advanced and accurate method to determine the parameters.

A. 500 kV Subpopulation Transformers

From table 2, Lognormal distribution and Weibull distribution are used in determining the remaining lifetime of this voltage subpopulation where TBF is the input data to the two distributions and the output will be failure rate and Reliability, respectively.

Figure 2, represents the failure rate where it is clear that failure rate increases by time, this concurs with ß is greater than 1 and failure rate increases by time, while, on the other hand, the failure rate of the Lognormal distribution increases till it reaches the peak values and then decreases by time [6, 10, 17]. Figure 3, represents the reliability of the transformers and remaining life time can be obtained at certain reliability rates. Reliability rates depend on the geographical factor; for example, area with industrial complexes may require a high-level reliability other than different areas.

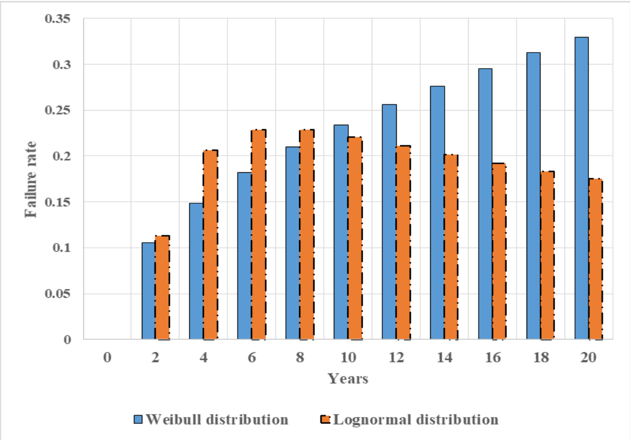

Fig .2 Failure rates of different probability distributions for 500 kV subpopulation

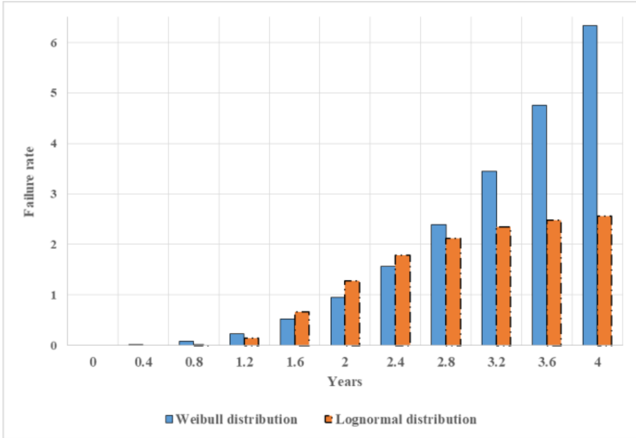

Fig .4 Failure rates of different probability distributions for 220 kV subpopulation

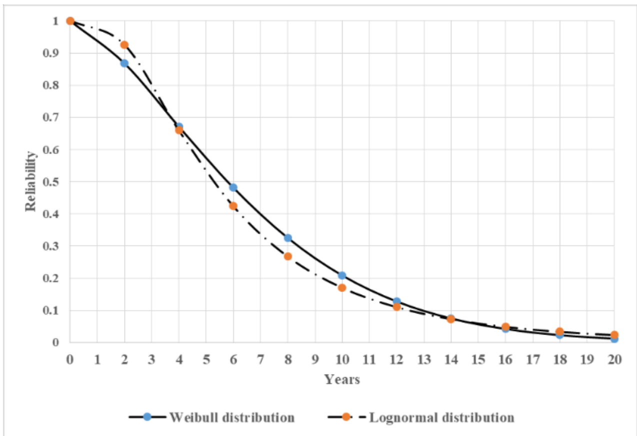

Fig .3 Reliability of different probability distributions for 500 kV subpopulation

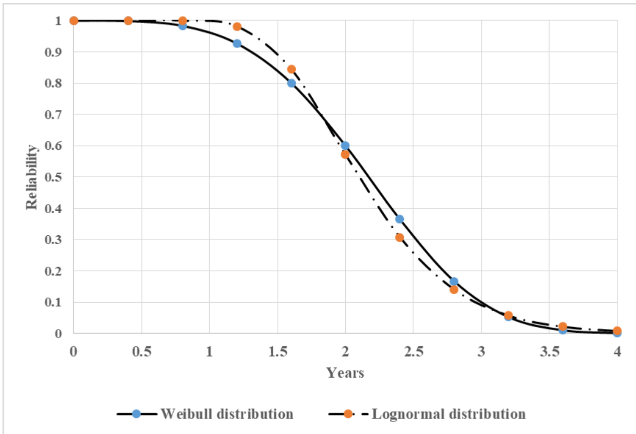

Fig .5 Reliability of different probability distributions for 220 kV subpopulation

B. 220 kV Subpopulation Transformers

This section focuses on 220 kV population transformers reliability and remaining life time through the same steps that were used in the 500-kV population.

Figure 4 indicates that failure rate regarding Weibull distribution increases rapidly by time while failure rate of Lognormal distribution reaches its peak at 4 years thus leads to the conclusion that the transformers must be replaced. Figure 5 illustrates the reliability through 4 years in which the remaining life time of the transformers is exploited.

C. 132 kV Subpopulation Transformers

This section focuses on 132 kV population transformers reliability and remaining life time through the same steps that were previously used in the 500 kV and 220 kV populations.

Figure 6 shows that the failure rate increases by time regarding Weibull distribution, but it increases at slow rate while. On the other hand, the curve of the failure rate resulting from lognormal distribution started from peak and then decreases by time. Figure7 shows that the reliability of both distributions in 50 years life span and reliability decreases gradually. However, reliability of Lognormal distribution decreases faster than that of Weibull distribution.

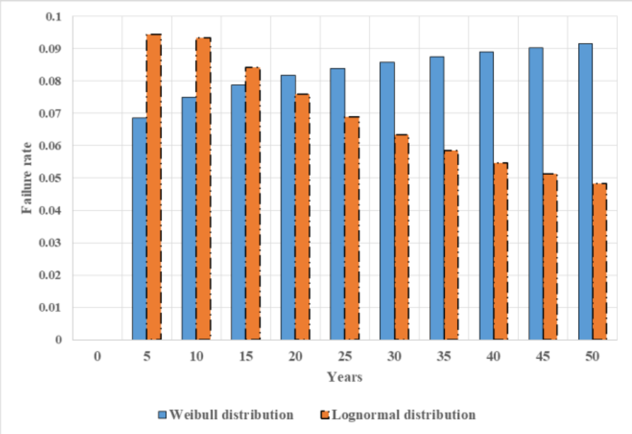

Fig .6 Failure rates of different probability distributions for 132 kV subpopulation.

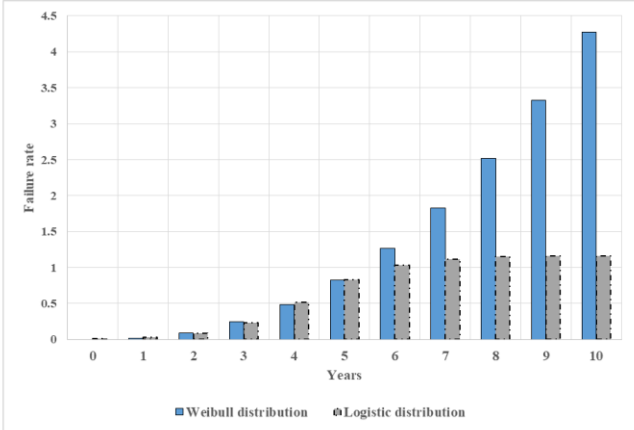

Fig .8 Failure rates of different probability distributions for 66-33 kV subpopulation.

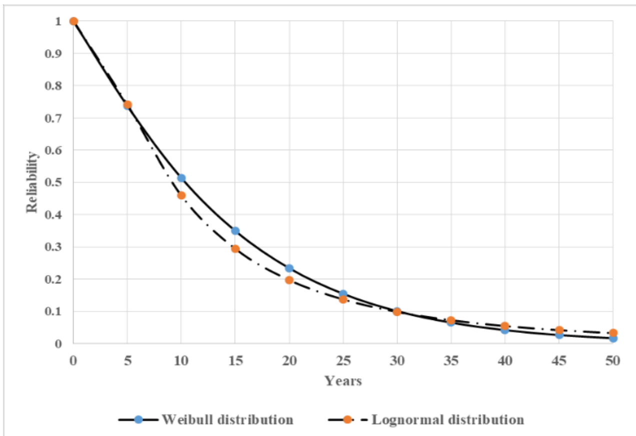

Fig .7 Reliability of different probability distributions for 132 kV subpopulation.

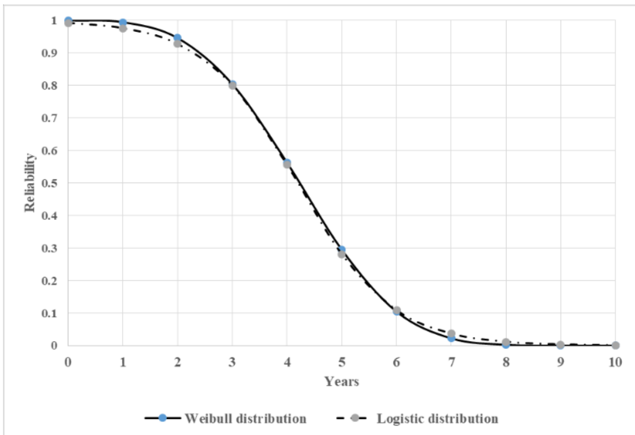

Fig .9 Reliability of different probability distributions for 66-33 kV subpopulation.

D. 66-33 kV Subpopulation Transformers

This section focuses on 66-33 kV population transformers reliability and remaining life time where the same steps that were used in the 500 kV, 220 kV and 132 kV populations are reused again. However, this is the only population that has used Logistic distribution instead of Lognormal distribution along with Weibull distribution based on the comparison of best fit distributions.

Figure 8 shows that failure rates of both distributions increase by time, this indicates that the transformers are in the wear out phase where failure rate increases rapidly regarding Weibull distribution and increases in a slow rate regarding Logistic distribution. Figure 9 shows that it is clear that reliability was decreasing slowly in the first 2 years then falls back till it reaches zero nearly at 8 years period of time and the transformers remaining life time can be obtained at certain reliability rates.

E. Transformers Availability Evaluation

This section discusses the availability (A) of the transformers of different voltage populations as availability can be calculated from (1) after determining TBFs and TTR as listed in appendix C [18]-[20].

$$A = \frac{TBFs}{TBFs+TTR} \quad (1)$$

Since (1) is per year, therefore for the whole 8 years study period, the mean time between failures (MTBF) and mean time to repair (MTTR) is used as in (2) .

$$A = \frac{MTBFs}{MTBFs+MTTR} \quad (2)$$

Figure 10 illustrates the different availability per year and for the overall study period for different voltage populations. In general, availability is high despite the increased failure rates and limited expected lifetime of transformers per voltage populations. From (2), the calculation for different voltage populations determined that 500 kV population has the lowest availability followed by 220 kV then 132 kV and finally 66-33 kV.

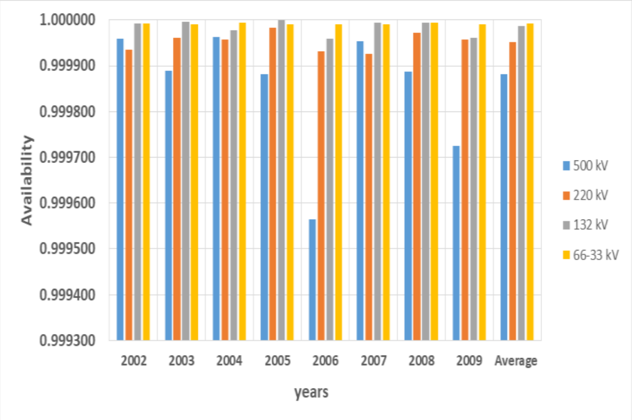

Fig .10 Different availability of different voltages population.

F. Results Discussion.

The results were based on 8 years study period and of course the longer the years the better the results will be, as transformers life span cab be of average 40-60 years [21, 22]. The results indicate that the transformers are in the wear-out phase of the bathtub curve for all voltage populations. Bathtub curve is a curve that describes 3 stages of any equipment. The first stage is the infant phase where the equipment starts operation for the first time with a low failure rate and high reliability. The second stage is the useful life phase where the failure rate is constant. The final phase is the wear-out phase in which the equipment operates for a long time, starts to fail at a certain point and needs replacing. In this phase, the failure rate increases and reliability decreases [4].

The remaining lifetime of the transformers for every voltage subpopulation is summarized in table 3 where the transformers in all voltages subpopulation must be replaced within few years with new transformers in order to deliver a higher reliability to the Egyptian power grid. Since Weibull distribution is common between all populations and is based on percentage difference of mean and STD, it is chosen to observe the remaining life time, where it is found that the remaining life span of the transformers in all populations is nearly alike and that the transformers will be expired with this range of years as shown in table (3). Choosing different reliability levels depends on the operator, while these voltage populations must have a high reliability level as these voltage populations exist in the transmission power system that delivers the generated electrical power to the distribution systems (low voltage system), thus these voltages are the only link between generation and distribution.

From the results, instructions can be delivered to the maintenance department in order to perform a proper maintenance schedule and to the operation department in order to operate and handle the transformers carefully. In addition, the results shall be sent to the manufacturer so that transformers with better components and with higher quality and technology are manufactured. This will lead to lowering the interruption power and lower repair time and customer interruption costs in which the costs were highly based on an earlier study of the same period of time to the transformers.

Table 3 Remaining Lifetime in Comparison between Different Voltage Populations.

Voltage Population / **Remaining Lifetime in Years**	**500 kV**	**220 kV**	**132 kV**	**66-33 kV**
Weibull distribution at 90 % Reliability level	1.6 years	1.3 years	2 years	2.4 years
Weibull distribution at 80 % Reliability level	2.7 years	1.6 years	3.75 years	3 years
Weibull distribution at 70 % Reliability level	3.7 years	1.8 years	5.75 years	3.45 years

3. G. Subassemblies Data Analysis.

As transformers are the most important equipment in the power system, analysis of their function, maintenance and observation reports are taken into consideration by the manufactures in order to deliver a much higher quality next generation transformers. [23, 24] mentioned the basis of the transformers design, protection, operation and maintenance.

There are 16 subassemblies of failures in which the analysis is applied [1]-[3]. These failures are sometimes referred to as outage causes and categorized into five categories which are transformer related outages, power system related outages, environment related outages, human factor related outages (HM), and unclassified/No flag (NF) and other outage causes. The transformer related outages are Buchholz and pressure relief (B&P), over current protection (OC), earth fault protection (EFP), differential protection (DP), breakdown and damage (B&D), firefighting system (FFS), hotspots (HS), leakage of SF6 or oil (leakage), and flash over (FO). The power system related outage category includes the outage of incomers (OI), and bus bar protection (BBP) actions. The environment related outage category includes bad weather (BW), and animal and birds (A&B) caused outages

A. Estimation of Remaining Lifetime for Each of the Subassemblies

Similar to the steps taken in order to estimate the remaining lifetime of the transformers, TBFs of different subassemblies are calculated and listed in table 4. Then the mean time between failures for every subassembly will be determined and compared to the mean time between failures for the whole transformer for different voltage populations. Finally, the remaining lifetime for every subassembly is estimated using Weibull distribution.

Table 4 and Figure 11 compare between MTBFs for every subassembly and for different voltage populations. It is clear that there is no direct relation between the overall MTBFs of the transformers as a complete set and the different subassemblies. A comparison is made to determine the Maximum and Minimum MTBFs for every subassembly for different voltage populations as shown in table 5. This comparison is made by excluding NF and other failures as they are not physical but undetermined failures. Table 5 also shows that that every voltage population has a different maximum and minimum values regarding MTBFs depending on number of failures and repair time.

Table 4 TBFs for Every Subassemblies Regarding 500 kV Population.

Voltage Populations	**500 kV**	**220 kV**	**132 kV**	**66-33 kV**
	Mean Values	Mean Values	Mean Values	Mean Values
TBF for whole transformer	6.60	2.17	13.67	4.22
TBF for B&P	1.33	71.99	9.88	86.42
TBF for OC	9.38	11.50	22.93	19.28
TBF for EFP	13.25	54.13	36.13	45.49
TBF for DP	13.25	21.21	34.42	37.19
TBF for B&D	15.00	39.31	28.69	62.72
TBF for FFS	15.25	106.5	10.63	340.2
TBF for HS	0.00	95.07	0.00	0.00
TBF for Leakage	7.63	22.14	8.27	0.00
TBF for FO	0.00	77.00	0.00	0.00
TBF for OI	0.00	73.46	18.71	15.01
TBF for BBP	3.75	86.59	3.33	438.5
TBF for BW	7.50	92.46	3.54	580.4
TBF for A&B	0.00	106.7	34.50	582.9
TBF for HM	0.00	34.09	5.19	735.3
TBF for NF	5.63	76.81	10.00	134.4
TBF for Others	15.75	15.63	13.16	197.6

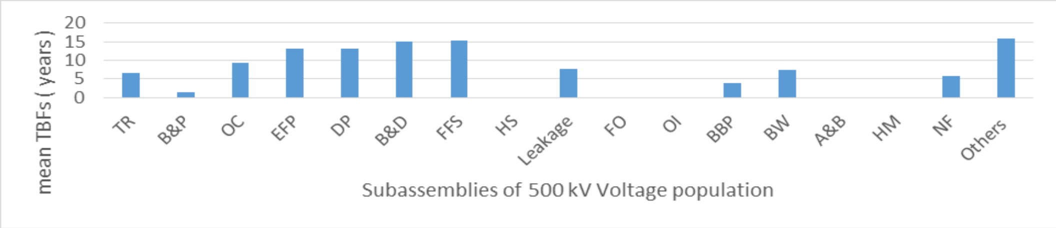

Fig . 11a. MTBFs for every subassembly regarding 500 kV population.

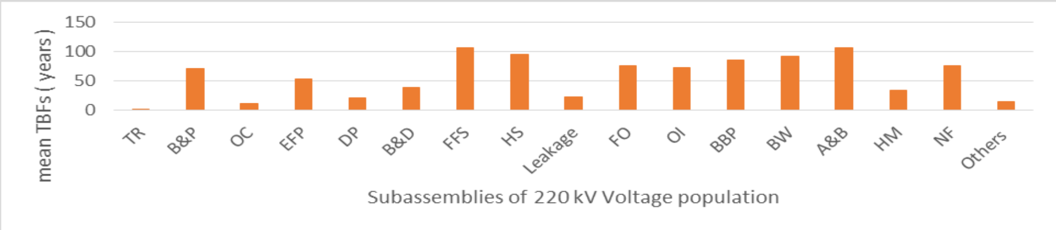

Fig . 11b. MTBFs for every subassembly regarding 220 kV population.

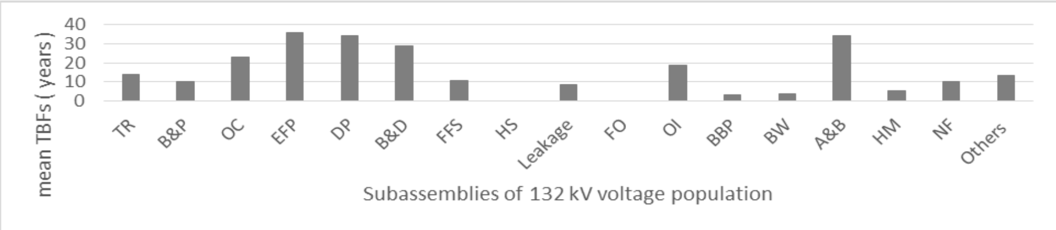

Fig . 11c. MTBFs for every subassembly regarding 132 kV population.

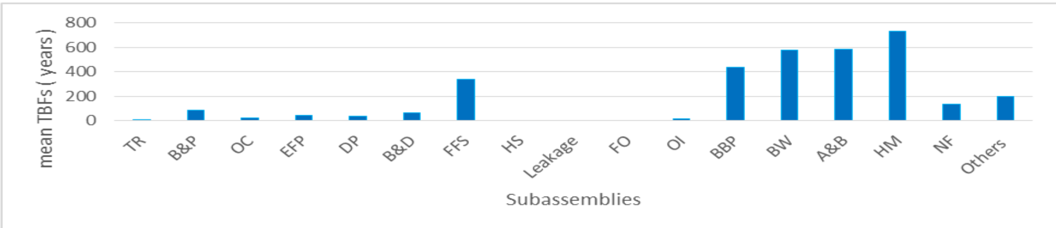

Fig . 11d. MTBFs for every subassembly regarding 66-33 kV population.

Table 5 Maximum and Minimum MTBFs for Different Voltage Population.

	500 kV	220 kV	132 kV	66-33 kV
Maximum MTBFs	B&D	FFS	EFP	HM
Minimum MTBFs	B&P	OC	BBP	OI

B. Results Discussion

The overall TBF of the whole transformer does not depend on the TBF of every subassembly. In fact, every subassembly has its own TBF that depends on different variables. For every subassembly, the components can be used for other purposes after the shutdown of the transformer such as bus bars, as bars can be recycled into new ones, or in case the failure did not affect their functionality. As shown in Figure 11, a comparison between different voltage populations is performed in order to check the MTBF among different subassemblies where MTBF differs from voltage population to another as it depends on the number of failures and the number of transformers. MTBFs indicates that the failure rate decreases as MTBF increases and vice versa as the TBFs decreases the failure rate increases.

Number of Failures, repair time and CIC per transformer analysis can provide solid data in order to improve maintenance schedules, inform the transformers' manufactures to enhance the quality of materials by performing more tests and offering training courses to the employees to reduce human error.

IV. CONCLUSIONS

This paper handled RAM analysis for the transformers of different voltage populations in the Egyptian power grid and the results showed that the transformers are

http://dx.doi.org/10.21622/RESD.2019.05.2.046

in the wear out phase but the availability of the transformers is high. This leads to enhancing maintenance schedules, improve the manufacturing process and train more personals.

Table 6 Remaining Lifetime for Every Subassembly in Different Voltage Populations.

500 kV		220 kV		132 kV		66-33 kV	
Subassembly	Remaining lifetime at 90 % reliability (years)	Subassembly	Remaining lifetime at 90 % reliability (years)	Subassembly	Remaining lifetime at 90 % reliability (years)	Subassembly	Remaining lifetime at 90 % reliability (years)
B&P	Occurred once	B&P	12.5	B&P	Occurred once	B&P	53.5
OC - 3 years study period	16.5	OC	8	OC - 6 years study period	6.5	OC	8.25
EFP - 4 years study period	20.25	EFP	5.5	EFP - 4 years study period	52.5	EFP	26.5
DP - 4 years study period	20.25	DP	15.5	DP - 6 years study period	23.5	DP	23.25
B&D - 4 years study period	This failure is constant at 30 years TBF	B&D	10	B&D - 4 years study period	28.5	B&D	30.5
FFS - 6 years study period	10.5	FFS	26.5	FFS	Occurred once	FFS	96.5
HS	No failures occurred	HS	18	HS	No failures	HS	No failures
Leakage - 3 years study period	11.25	Leakage	13.75	Leakage - 2 years study period	24.75	Leakage	No failures
FO	No failures occurred	FO	38	FO	No failures	FO	No failures
OI	No failures occurred	OI	15	OI - 5 years study period	12.75	OI	5.75
BBP	Occurred once	BBP	10	BBP	Occurred once	BBP – 7 years study period	84.5
BW - 2 years study period	This failure is constant at 30 years TBF	BW	29.5	BW	Occurred once	BW - 7 years study period	134
A&B	No failures occurred	A&B	75	A&B - 4 years study period	40.5	A&B - 7 years study period	184
HM	No failures occurred	HM	26	HM	Occurred once	HM	188
NF - 2 years study period	13	NF	17	NF	Occurred once	NF	72.5
Others - 6 years study period	9.25	Others	10.25	Others - 2 years study period	15.5	Others	85.5

REFERENCES

[1] M. Abdelfatah , M. El-Shimy , and H.M. Ismail. “Outage data analysis of utility power transformers based on outage reports during 2002–2009,” International Journal of Electrical Power & Energy Systems, vol. 47, pp. 41-51, May, 2013.

[2] M. Abdelfatah , M. EL-Shimy, and H.M. Ismail. “Reliability and maintainability analysis of medium voltage transformers in Egypt,” in The 8th International Conference on Electrical Engineering (ICEENG-8) of the Egyptian Military Technical College, Cairo, Egypt, 2012, pp. 1-17.

[3] M. EL-Shimy , M. Abdelfatah , and H.M. Ismail. “Reliability, availability, and maintainability (RAM) analysis of utility power transformers in Egypt,” ELEKTRIKA-UTM Journal of Electrical Engineering, Vol. 14, no. 1, pp. 1-5, Jan. 2012.

[4] Life Data Analysis erence, ReliaSoft Corporation [On-line] Available: http://www.ReliaSoft.com [Jan. 5, 2018].

[5] R.B. Abernethy, J.E. Breneman, C.H. Medlin, G.L. Reinman. Weibull analysis handbook. Pratt and Whitney West Palm beach fl Government Products, DIV, 1983.

[6] W.B. Nelson. Applied life data analysis. Place of publication: John Wiley & Sons, 2005.

[7] C. Forbes, M. Evans, N. Hastings, and B. Peacock. Statistical distributions. Place of publication: John Wiley & Sons, 2011.

[8] Life Data Analysis erence, ReliaSoft Corporation [On-line] Available: http://www.ReliaSoft.com [Jan 5, 2018].

[9] Oracle help center [online] Available: https://docs.oracle.com/cd/E12825_01/epm.111/cb_user/frameset.htm?apas04.html [Jan 5, 2018].

[10] W.G. Ireson, C.F. Coombs, R.Y. Moss. Handbook of reliability engineering and management. Place of publication: McGraw-Hill Professional, 1996.

[11] J. Mun. Advanced analytical models: Over 800 models and 300 applications from the Basel II accord to Wall Street and beyond. Place of publication: John Wiley & Sons, 2008,, appendix C.

[12] Online Help Manual, MATLAB Cooperation [On-line] Available: https://www.mathworks.com/help/stats/rayleigh-distribution.html [Mar. 3, 2018].

[13] R.B. Abernethy. The New Weibull handbook: Reliability and statistical analysis for predicting life, safety, supportability, risk, cost and warranty claims. North Palm Beach, FL: Dr. Robert B. Abernethy, 2004.

[14] D. Martin, J. Marks, T.K. Saha, O. Krause, and N. Mahmoudi. “Investigation into modeling Australian power transformer failure and retirement statistics,” IEEE Transactions on Power Delivery, vol, 33, no. 4, pp. 2011-9, Aug. 2018.

[15] Online Help Manual, MATLAB Cooperation [On-line] Available: https://www.mathworks.com/help/stats/wblfit.html [Mar. 3, 2018].

[16] Online Help Manual, MATLAB Cooperation [On-line] Available: https://www.mathworks.com/help/stats/weibull-distribution.html [Mar. 3, 2018].

[17] A.D. Telang, V. Mariappan. “Hazard rate of Lognormal distribution: An investigation,” International Journal of Performability Engineering, vol. 4, no. 2, pp. 103, Apr. 2008.

[18] M.F. Aly, I.H. Afefy, R.K. Abdel-Magied, and E.K. Elhalim, “A comprehensive model of reliability, availability, and maintainability (RAM) for industrial systems evaluations,” JJMIE, vol. 12, no. 1, pp. 59-67, Jun. 2018.

[19] S. Verbrugge, D. Colle, P. Demeester, R. Huelsermann, and M. Jaeger. “General availability model for multilayer transport networks,” in DRCN 2005. Proceedings. 5th international workshop on design of reliable communication networks, IEEE, Oct. 2005, pp. 85-92.

http://dx.doi.org/10.21622/RESD.2019.05.2.046

[20] E. Vargas. “High availability fundamentals.”, Sun Blueprints series. 2000 Nov: 1-7. California, USA Nov.2000, pp. 1-17.

[21] P. Jarman, R. Hooton, L. Walker, Q. Zhong, T. Ishak, and Z. Wang. “Transformer life prediction using data from units removed from service and thermal modelling,” in Proc. CIGRE Session, 2010, pp. 1-7.

[22] P. Jarman, Z. Wang, Q. Zhong, and T. Ishak, “End-of-life modelling for power transformers in aged power system networks,” in CIGRE 2009 6th Southern Africa regional conference, Cape Town, Southern Africa, 2009 Aug 17, pp.1-7.

[23] Bureau of RECLAMATION “Transformers: Basics, maintenance and diagnostics,”, US Department of the Interior Bureau of Reclamation. Denver, Colorado, USA. Apr. 2005.

[24] J.H. Harlow. “Electric power transformer engineering,”, CRC press; New York, USA, Dec. 2011

Journal of Renewable Energy and Sustainable Development (RESD) Volume 5, Issue 2, December 2019 - ISSN 2356-8569
http://dx.doi.org/10.21622/RESD.2019.05.2.057

Modelling and Energy Analysis of Solid Oxide Fuel Cell (SOFC) Operated by the PV System in the Residential Sector in Australia

Scarlett Allende
Los Zarzales 1533, Santiago 9270842. Chile,
ssallend@uc.cl

***Abstract* -** This paper presents an energy evaluation of a hybrid system composed of a photovoltaic farm, hydrogen consumption and solid oxide fuel cell, which simulation involves the electric demand of a household in the Western territory of Australia. Specifically, the study evidences a significant solar potential that provides 4659kWh/year. However, there is an energy deficit in the period when the load energy is higher than the solar generation. As a result, the fuel cell integration solves the irregularities of solar availability, providing 4567kWh/year load demand and 477827kWh/year of energy delivered to the grid. Finally, the configuration of the system generates 50% more than the energy required, which allows enlarging the electric consumption and the possibility to append thermal energy.

***Keywords* -** Hybrid system, Fuel cell, Photovoltaic, Hydrogen, Residential sector, Energy demand.

I. INTRODUCTION

The primary purpose of this study is to know the potential of the natural sources of Western Australia, determine the electricity and hydrogen demand, analyse the integration of the fuel cell into PV system and evaluate the hybrid system performance. Overall, Australia presents a significant development in the renewable energies due to natural resources available and the target of clean energy regulation existing in different states [1]. Particularly, WA has a relevant potential in renewable's energies, particularly in solar households with 27% of capacity (rooftop solar technology) [2].

The high solar radiation in Australia allows getting progress in the industry, especially in the desert areas (northwest and centre), resulting in total solar radiation of 58 million PJ. Also, due to the policies of clean energy, the government expects to generate 1000MW from solar power, promoting the capacity of electric and thermal technologies, though, the current production of solar energy denotes 0.1% of the total primary energy demand [3]

At the same time, Australia has expanded the type of renewable resources, such as the hydrogen industry that allows exploring new technologies, including fuel cell development. Specifically, the implementation of the fuel cell as an electric generator provides a reliable energy system due to the option of seasonal hydrogen storage and grid stability. Furthermore, it's an alternative to remote area power systems [4].

II. METHODOLOGY

A. Estimating Energy Demand

The annual electric demand was calculated considering the simulator plan of Australian energy consumption [5]. The study understands factors that influence electrical use, such as the location, number of people living in the house and the usage of facilities. Specifically, the simulation applied in this paper involved the electric consumption of two people, which includes the pool facilities and slab heating system. Equivalently, the daily and hourly use were calculated based on the periods of electric usage, considering the distribution of the energy plan simulation on the 8760 hours per year.

1. Photovoltaic farm

The solar research was in the coordinates -25.69, 116.2, which corresponds to the Western territory of Australia. The first step of the study involved obtaining the monthly data of temperature and solar irradiation, extracted from the photovoltaic geographical information system [6]. These data correspond to the average hourly of air temperature [°C] and the global and diffuse radiation [kWh/m^2] of each month. Considering these last two data was possible to estimate the slope radiation [kWh/m^2]. Fig. 1 explains the sequence of steps done on this methodology.

It is important to note that Fig. 1 is modified from a similar study [7], where the hourly global and diffuse solar irradiation (kWh/m^2) were from the NASA database. However, this research considered the PVGIS Explorer data. The rest of the steps follows the same logic. The resulting diagram explains the sequence of the steps done on this methodology.

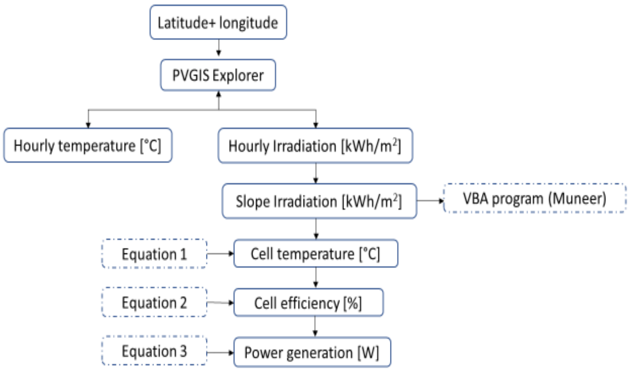

Fig .1 Calculation method for the power generation of one PV module. Modified from [7].

The cell temperature, efficiency and power generation of one photovoltaic module were calculated considering Equation 1, 2 and 3. Mainly, the factors are represented by the air temperature obtained from the PVGIS Explorer (Ta); global slope irradiation (Gslope); global radiation at the nominal operating cell temperature (Gnoct); nominal operating PV cell temperature (Tc, noct) [8]; cell efficiency at standard test conditions (nstc); absorptivity of the module (Tα); cell temperature at standard testing conditions (Tc, stc); temperature coefficient value (αp) [9]; electrical efficiency at standard test conditions (η mod) and area of the PV module surface (A). It is essential to note that some values of the formulas belong to the database of the PV module [10].

$$\mathrm{Tc} = \mathrm{Ta} + \left(\frac{\mathrm{Gslope}}{\mathrm{Gnoct}}\right)(\mathrm{Tc,noct} - \mathrm{Ta,noct})\left(1 - \left(\mathrm{n}\frac{\mathrm{stc}}{\mathrm{T\alpha}}\right)\right)[°C]$$

Eq .1: Cell temperature of PV panel [8].

$$\eta cell = \eta stc\ [1 + \alpha p(Tc - Tc, stc)]\ [\%]$$

Eq .2: Cell efficiency of a photovoltaic module [8].

$$P = \eta mod * A * Gtlt\ [1 - 0.0045Tc - 298.15][W]$$

Eq .3: Power generation of PV panel [7].

Then the solar farm is determined by the relation between the total electric demanded and the energy provided by a single PV panel. The last function is represented by Equation 4, where Am is the useful area of the photovoltaic module and Itilt is the tilted global irradiance.

$$E\ module = Am * \eta stc * Itilt\ [kWh/day]$$

Eq .4: Energy of one photovoltaic panel [11].

2. Integration photovoltaic-fuel cell system

Firstly, it was necessary to estimate the hydrogen consumption of the hybrid system. As a result, Equation 5 describes the factors involved, such as the yearly electric demand (E_demand); efficiency of the PV-H2-SOFC system and higher heating value of the hydrogen (HHV).

$$H2_{demand} = \frac{E\_demand}{Efficiency * HHV}[kg]$$

Eq .5: Amount of hydrogen required in the hybrid system [12].

After getting the energy demand, solar source and hydrogen consumption, it was possible to simulate the system by the FCPower model [13]. Additionally, it was necessary to include types of equipment data specification, such as from the PV panel, electrolyser [14] and fuel cell [15] used in the simulation. Details of the modelling process are explained in Fig. 2.

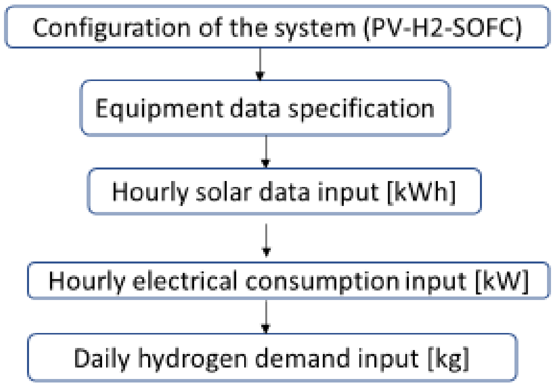

Fig .2 Flow diagram of the FCPower simulation according to the hybrid system configuration [7].

III. RESULTS

A. *Solar Radiation and Air Temperature*

According to the database from the photovoltaic geographical information system (PVGIS), the air temperature values consider the hourly temperature average of each month, corresponding to the year 2016. Notably, the maximum and minimum temperature variation during the year was in November and June with around 14°C and 9°C of difference, respectively. The result of the simulation is detailed in Table 1.

Table 1 Summary of the Monthly Ambient Temperature [6]

Month	Average [°C]	Max [°C]	Min [°C]
Jan	30.83	37.7	25
Feb	31.60	37.8	26.1
Mar	29.46	35.1	24.3
Apr	25.45	30.8	20.7
May	20.89	26.2	16.4
Jun	17.16	22	13.5
Jul	16.09	21.2	12
Aug	18.22	24	13.2
Sep	20.10	26.1	14.5
Oct	23.58	30.2	17.2
Nov	26.03	33	19.4
Dec	28.59	35.4	22

Analogously, the simulation provides hourly and monthly global horizontal radiation. Table 2 indicates that during December produce the highest solar potential with over 800 [W/m^2], between the 11 and 15 hours. In contrast, the lowest radiation was in wintertime (June and July), with less of 200 [W/m^2].

B. Cell Temperature, Efficiency and Output Power

Based on the air temperature values, factors and formulas it was possible to obtain the monthly and hourly cell temperature. The result per month showed that the PV panel increases the heat during the summer season, approximately 2°C. At the same time, Fig. 3 describes the result per hour, where the rise appears in the afternoon, with around 3°C of difference.

Table 2 Average of the Global Radiation Per Hour and Month [W/m^2]

Hour/month	Jan	Feb	Mar	Apr	May	Jun	Jul	Aug	Sept	Oct	Nov	Dec
0	0	0	0	0	0	0	0	0	0	0	0	0
1	0	0	0	0	0	0	0	0	0	0	0	0
2	0	0	0	0	0	0	0	0	0	0	0	0
3	0	0	0	0	0	0	0	0	0	0	0	0
4	0	0	0	0	0	0	0	0	0	0	0	0
5	0	0	0	0	0	0	0	0	0	0	0	0
6	0	0	0	0	0	0	0	0	0	0	27	22
7	47	8	8	0	0	0	0	0	15	95	188	194
8	129	185	210	72	56	49	46	60	201	376	537	567
9	124	257	263	141	64	52	51	89	254	412	560	578
10	157	385	396	245	123	75	88	186	374	547	690	722
11	163	488	495	331	191	129	153	264	460	639	777	821
12	160	552	550	375	235	169	198	313	506	684	821	865
13	162	564	564	386	237	176	204	323	511	682	817	864
14	173	517	535	354	210	152	184	296	472	631	764	821
15	191	425	468	290	150	101	132	235	398	541	667	719
16	162	344	360	196	86	77	82	149	293	417	544	608
17	134	219	224	92	50	37	46	71	170	271	396	465
18	92	125	104	19	0	0	0	15	47	108	224	304
19	38	20	0	0	0	0	0	0	0	0	1	90
20	0	0	0	0	0	0	0	0	0	0	0	0
21	0	0	0	0	0	0	0	0	0	0	0	0
22	0	0	0	0	0	0	0	0	0	0	0	0
23	0	0	0	0	0	0	0	0	0	0	0	0

On the other hand, the relationship between the PV, the cell temperature and the cell efficiency are represented by Fig. 4 and 5. Principally, this last variable decreases during summer (January and February) with 15% less. Furthermore, the period with the lowest performance was between 13 and 15 hours, with almost 14.7% at 9°C.

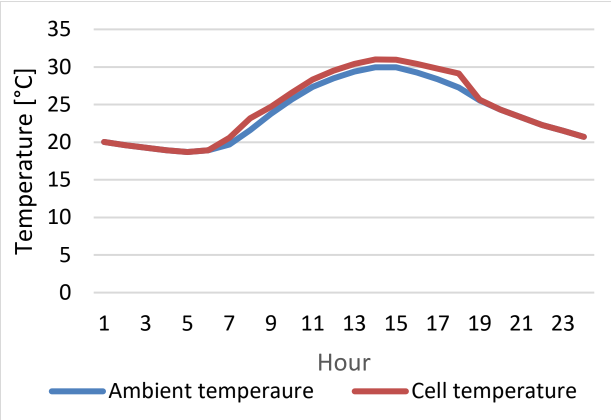

Fig .3 Average of ambient and cell temperature per hour.

At the same time, the power generation of the photovoltaic panel was calculated per hour and month, with results manifested in Table 3. Overall, the peak is concentred in intervals during mornings and evenings of the summer season. For example, December shows the highest power production at the 8 and 18 hours, with 221 and 284 W, respectively. In the rest of the months, the same variation exists but with a lower outpower.

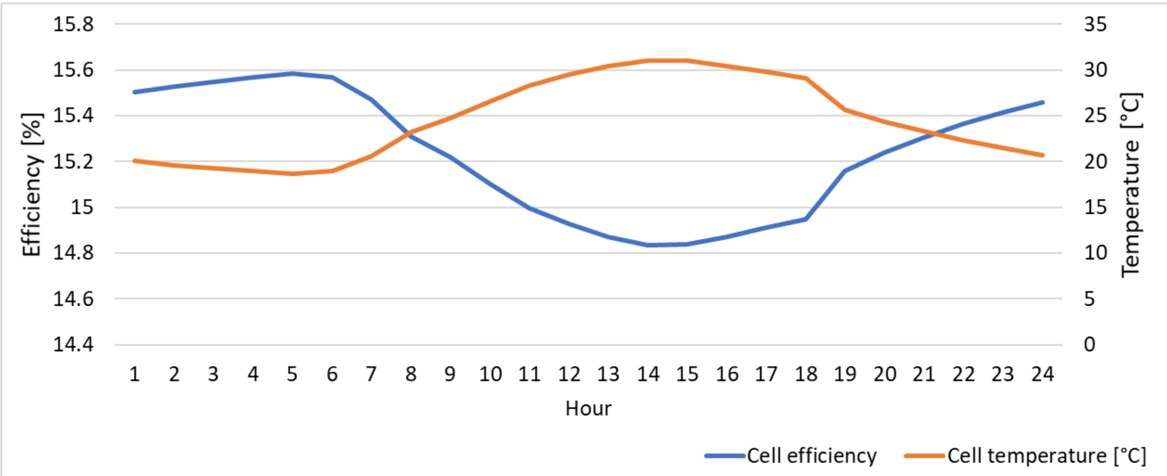

Fig .4 Cell temperature and Efficiency per month.

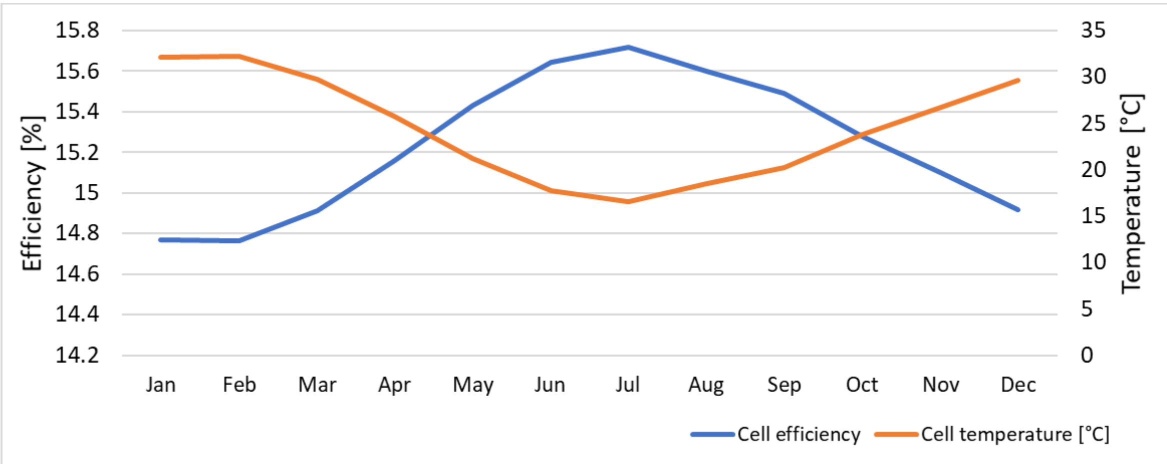

Fig .5 Average of the cell temperature and efficiency per hour.

C. Determination of PV System

Regarding the results calculated previously, it was possible to obtain the PV modules quantity required in the hybrid system. In this case, the annual electric demand extracted from the simulator plan of Australian energy consumption was of 4610 kWh. Additionally, the energy produced by one photovoltaic module was of 89.43 kWh/year. As a result, the total of modules was of 52. Details are in Table 4.

The energy generation of the solar farm was calculated considering the number of PV panels required, and the energy produced by a single photovoltaic module. This last find was around 90kWh/year. In contrast, the global supplied was of 4659kWh/year, which includes the energy generation of 52 PV panels. As Table 5 shows, the month with the highest energy production was December with 996kWh, and the lowest was June with 162kWh.

Table 4 Summary of the Monthly Ambient Temperature [6]

E panel kWh/day	E panel kWh//yr.	Total consumption , kWh/yr.	PV panels
0.245	89.43	4610	52

Table 3 PV Module Output Power [W].

Month/ Hour	Jan	Feb	Mar	Apr	May	Jun	Jul	Aug	Sep	Oct	Nov	Dec
1	0.0	0.0	0.0	0.0	0.0	0.0	0.0	0.0	0.0	0.0	0.0	0.0
2	0.0	0.0	0.0	0.0	0.0	0.0	0.0	0.0	0.0	0.0	0.0	0.0
3	0.0	0.0	0.0	0.0	0.0	0.0	0.0	0.0	0.0	0.0	0.0	0.0
4	0.0	0.0	0.0	0.0	0.0	0.0	0.0	0.0	0.0	0.0	0.0	0.0
5	0.0	0.0	0.0	0.0	0.0	0.0	0.0	0.0	0.0	0.0	0.0	0.0
6	0.0	0.0	0.0	0.0	0.0	0.0	0.0	0.0	0.0	0.0	2.6	2.0
7	71.9	14.8	2.2	0.0	0.0	0.0	0.0	0.0	5.6	36.9	138.8	165.7
8	164.1	67.5	25.7	16.1	20.6	17.9	16.8	20.6	30.6	39.9	139.6	220.6
9	84.5	35.9	29.3	22.1	18.8	19.1	18.7	15.5	28.0	40.9	50.3	111.1
10	50.5	45.8	37.2	30.6	21.7	22.7	21.7	23.7	38.2	49.1	48.4	61.5
11	53.7	49.1	42.5	37.6	27.0	25.7	26.7	28.0	39.9	49.4	50.1	50.4
12	52.7	50.1	42.5	37.9	32.3	30.3	31.0	31.3	39.5	49.8	49.8	53.1
13	53.4	51.7	45.1	39.9	31.3	30.6	30.3	31.3	39.9	49.8	51.7	54.4
14	57.0	55.7	48.8	38.6	31.0	29.7	31.0	30.0	37.6	51.4	53.4	56.0
15	58.3	58.7	46.1	36.6	26.4	25.0	27.0	28.0	34.3	47.8	53.4	68.9
16	100.8	49.8	38.9	29.0	22.4	28.0	24.7	22.7	29.3	40.9	53.3	117.5
17	158.4	66.2	31.0	18.5	17.9	13.5	17.2	18.8	25.0	32.3	109.2	182.8
18	249.2	131.3	19.8	8.4	0.0	0.0	0.0	6.9	15.4	42.2	172.4	283.6
19	21.5	9.9	0.0	0.0	0.0	0.0	0.0	0.0	0.0	0.0	0.0	18.1
20	0.0	0.0	0.0	0.0	0.0	0.0	0.0	0.0	0.0	0.0	0.0	0.0
21	0.0	0.0	0.0	0.0	0.0	0.0	0.0	0.0	0.0	0.0	0.0	0.0
22	0.0	0.0	0.0	0.0	0.0	0.0	0.0	0.0	0.0	0.0	0.0	0.0
23	0.0	0.0	0.0	0.0	0.0	0.0	0.0	0.0	0.0	0.0	0.0	0.0
24	0.0	0.0	0.0	0.0	0.0	0.0	0.0	0.0	0.0	0.0	0.0	0.0

The design of PV facilities is composed of six rows and seven columns of panels with 45° inclination and orientated towards the north. Nevertheless, to reduce the shadow risk, the PV arrows have a prudent distance between them. Furthermore, the sizing of PV array considers two inventers for the total of modules. Fig. 7 shows the solar farm involved and location. Principally, the area distribution includes two aspects; the first one is a useful area that represents the location of the panels, with 322m^2. The second factor is around 30% more surface (419m^2) intended to a maintenance purpose in the system.

Similarly, Fig. 6 illustrates the distribution of energy consumption and the energy supplied. The electric demand showed steady rises and drops. However, there are significant leaps of the energy provided by the solar system, especially in December. Comparatively, during wintertime, the energy demand was higher than the produced. However, this has switched drastically in summer.

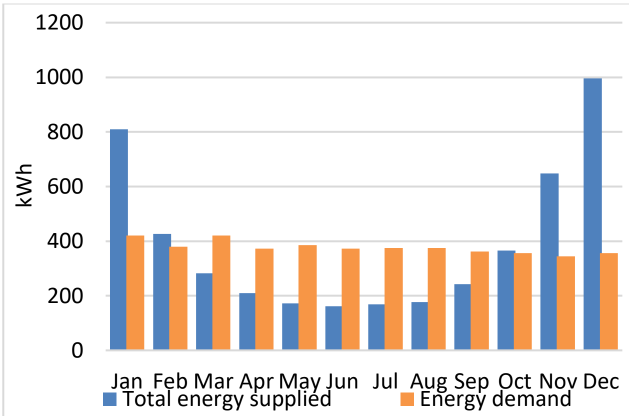

Fig .6 Comparison between the energy demand and the energy supplied by the solar farm.

The array size involves a voltage dimension of 60V and 49V for the respective maximum and minimum open circuit voltage. Furthermore, the maximum current in the photovoltaic module was of 8.4A. Analogously, the interval of PV modules per string was between 10 and 5, considering a maximum of voltage and current per line of 600V and 18A, respectively.
The design of PV facilities is composed of six rows and

http://dx.doi.org/10.21622/RESD.2019.05.2.057

seven columns of panels with 45° inclination and orientated towards the north. Nevertheless, to reduce the shadow risk, the PV arrows have a prudent distance between them. Furthermore, the sizing of PV array considers two inventers for the total of modules. Fig. 7 shows the solar farm involved and location. Principally, the area distribution includes two aspects; the first one is a useful area that represents the location of the panels, with 322m^2. The second factor is around 30% more surface (419m^2) intended to a maintenance purpose in the system.

Table 5 Summary of Output Energy of Photovoltaic Module.

Month	Energy single module supplied [kWh]	Total Energy module supplied [kWh]
Jan	15.57	809.8
Feb	8.21	426.9
Mar	5.42	281.8
Apr	4.04	210.0
May	3.3	171.7
Jun	3.10	161.7
Jul	3.25	168.8
Aug	3.40	176.9
Sep	4.66	242.1
Oct	7.02	365.1
Nov	12.47	648.4
Dec	19.15	995.5
Total	89.589	4658.678

Fig .7 Location of solar farm. Source: (Google earth, 2019).

D. Configuration of the PV-H2-SOFC System.

The first stage of the hybrid system design involves the solar energy that provides electric generation and hydrogen for the fuel cell system. However, if the hydrogen production is not enough to supply the demand of the system, it is necessary to add the missing hydrogen from an external source. As a result, the PV-H2-SOFC configuration has two parties, one from solar energy providing the hydrogen partially to the electrolyser, and the other from the hydrogen storage. As Fig. 8 describes, the first scenario exists when the PV generation is lower than the energy consumption.

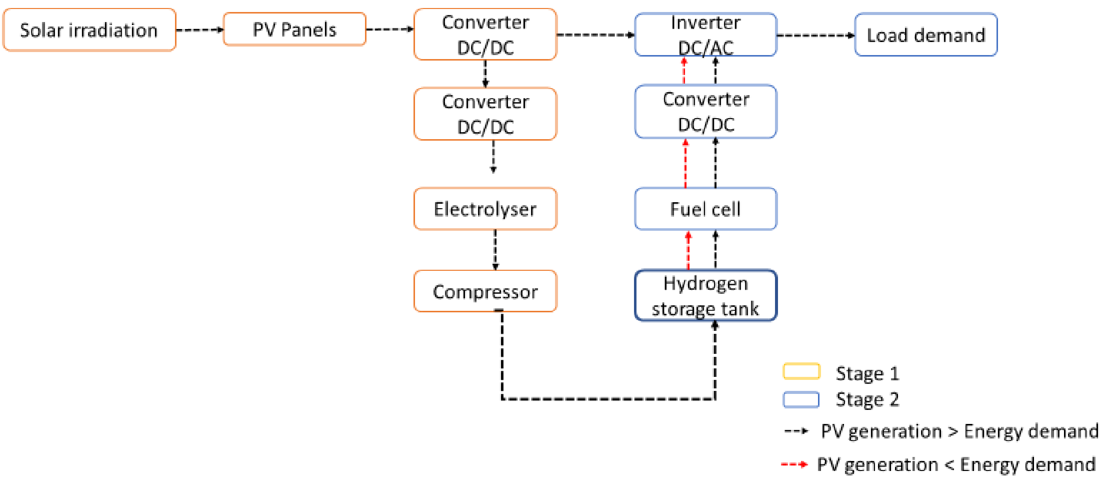

Fig .8 Design of PV-H2-SOFC system [7].

Based on the hydrogen calculation and the energy consumption, it was possible to get the comparative variation between both requirements. As Fig. 9 describes, the energy demand is proportional to the hydrogen consumption of the fuel cell. For example, the highest and lowest demand for hydrogen and electricity are during summer and spring, respectively. The range of both periods is between 660-780m^3 for the hydrogen and 1050-1200kWh for electric consumption.

On the other hand, according to the results of the hydrogen produced from PV generation and the hydrogen required, the deficit of hydrogen of the hybrid system was determined. In this case, the highest gap was in the wintertime, with 17.98kg missing hydrogen. In contrast, in the months of summer presented the lowest variation, with a deficit of 9.86kg. The hydrogen distribution is described in Fig. 10.

http://dx.doi.org/10.21622/RESD.2019.05.2.057

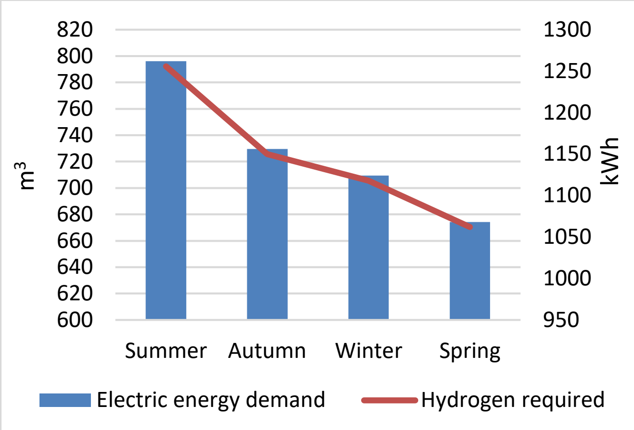

Fig .9 Hydrogen demand and electricity required per season.

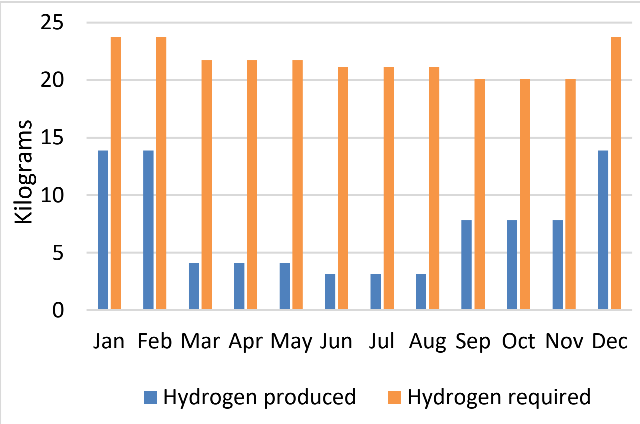

Fig .10 Hydrogen demand and hydrogen deficit per month.

The storage tank was dimensioned considering the highest deficit of hydrogen of the year (18kg/month and 200m³/month) and the values of volume and pressure of the electrolyser and tank. As a consequence, the hydrogen pressurised was 30.8m³, but for safety reasons, it must include a 10% of volume [16], with a final dimension tank of 33.88m³. It is important to note that the location of the tank was underground due to the reduced risk of temperature fluctuation [7].

E. Simulation Results.

The FCPower model provided the modelling results of the PV-H2-SOFC system, which started with the annual input specifications data, such as the solar capacity factor and the amount of fuel used in the fuel cell. For example, the yearly system energy output used onsite is the balance between the delivered of electricity (4567kWh), heat (0 kWh), hydrogen (8763kWh), and grid electricity to the building (0 kWh). Details of those values are presented in Table 6.

Table 6 Energy Input of the System, from FCPower Model Simulation [13].

Values	Specifications
86.801	Fuel used in FCS [kWh/kWh]
0.000	Fuel used in burner [kWh/kWh]
0.349	AC from solar [kWh/kWh]
0.000	AC from wind [kWh/kWh]
0.000	Purchased Grid Electricity [kWh/kWh]
0.0%	Purchased grid electricity cost (wtd avg % of base cost)
13,331	System Energy Output Used Onsite per Year [kWh]

At the same time, the model provides the general specification of the fuel cell, considering the range of energy capacity 53.3kWh; combined heat, hydrogen, and power efficiency of 63%; fuel consumed for combined heat and power of 132kWh and the maximum hydrogen generation of 17kW. Table 7 shows the data specification of the SOFC system.

Table 7 Summary of the Fuel Cell Specifications Per Hour [13].

Specification	Value	Units
Electricity Produced	53.33	kW
Electrical CHP efficiency at current electrical power level	0.4047	kW/kW
Total CHP efficiency at current electrical power level	0.6273	kW/kW
Fuel used for CHP operations	131.8	kW
CHP heat total	29.3	kW
Max H2 production ability	17.0	kW
Max H2 over-production ability	11.4	kW
H2 production	0.0	kW
CHP heat used for H2 production	0.0	kW
CHP heat out total	29.3	kW
Over-production of H2	0.0	kW
Fuel used for H2 over-production	0.0	kW
Total fuel consumption	131.8	kW

The hourly output results showed that the electricity delivery was of 0.343kWh per kWh produced by the hybrid system. Besides, the hydrogen delivery was 0.657kWh/kWh, which represents the relation between the hydrogen delivered and the yearly system energy output used onsite. Analogously, the electricity sold to the grid includes the results of the energy input (13331kWh/year), and the excess of energy intended to the grid (477827kWh). Table 8 details the total of power supplied by the PV-H2-SOFC system (491158kWh), which considers the values of electricity generated, energy sold, hydrogen production and heat delivered.

Table 8 Energy Output of the System, from FCPower Model Simulation [13].

Values	Specifications
0.343	AC Delivered [kWh/kWh]
0.000	Heat Delivered [kWh/kWh]
0.657	Hydrogen Delivered [kWh/kWh]
3.58E+01	AC sold to grid [kWh/kWh]
491,158	Total Energy Supplied per Year [kWh]

Finally, the simulation provided different types of efficiencies as explained in Fig. 11. Principally, the fuel cell efficiency was higher than the electrical performance; for example, in the operating fraction 0.5, the capabilities were 70% and 45%, respectively. Furthermore, the capacities of the categories of hydrogen-fuel-cell and electrolyser were significantly similar, with around 52% of the performance at 100% of operation.

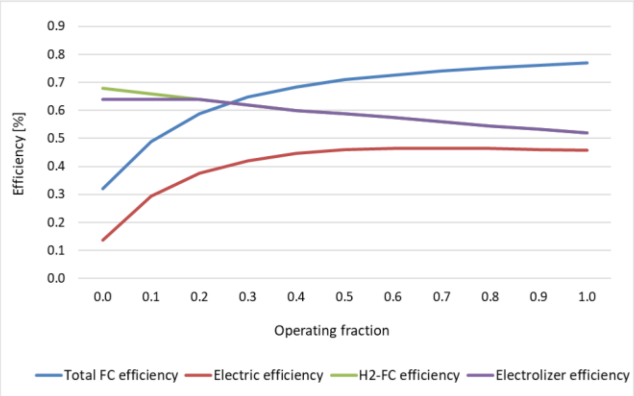

Fig .11 Performance of PV-H2-SOFC system. Modified from [13].

IV. ECONOMIC ANALYSIS

According to financial results obtained from FCPower model simulation, the price factors of system net electricity and hydrogen were 0.133 $/kWh and 35.7 $/kWh, respectively. As a result, considering 4567 kWh/year of electricity production from the hybrid system and 8763 kWh of hydrogen required, the total cost of energy generation was 313,446 $/year. However, this cost can be reduced, considering the system electricity sold to the grid of 38,912$/year, whose values includes 477,827 kWh/year of excess and the sold price factor of 0.081 $/kWh. The total cost obtained was 274,534 $/year. Analogously, the Australian electricity load price is around 0.22 $/kWh [17], which involves a total value of 913 $/year.

Overall, the electricity cost from the hybrid system was competitive compared to the grid (around 33% cheaper). Nonetheless, the deficit of hydrogen increases is considerable to the global cost.

On the other hand, one of the main advantages of fuel cell integration was the elimination electric battery into the hybrid system configuration due to the water electrolysis can solve the irregularity of solar availability. Therefore, its elimination helps to decrease the operational cost by around 30% [7].

V. CONCLUSION

According to the solar power generation, hydrogen and fuel cell modelling, the hybrid system is a viable alternative to supply the electric consumption of one house. Therefore, the following points summarise the findings:

- The Western territory of Australia showed an elevated solar source, considering that the highest daily average was in December with a global radiation of 318 W/m^2. The rest of the months presented a slight difference between them.

- The hourly variation between the cell efficiency and panel temperature did not change significantly as the performance was reduced by 0.2% in the 13 hours. However, the monthly results showed that the efficiency decreased by 1% during summertime.

- The solar farm can supply the total annual demand. Nevertheless, the distribution of electricity generation was significantly unequal. For example, in the wintertime, solar energy only provides 47% of the total consumption required. As importantly, the integration of the fuel cell helps to supply this deficit.

- The electricity generation increases by more than 30% with the integration of the fuel cell. Specifically, the photovoltaic energy produced 4658kWh/year, and the solid oxide fuel cell generated 4567kWh/year of electricity load and 477827kWh/year of delivered to the grid. As a result, both renewables sources are 9225kWh/year, which represents 50% more than the energy demand.

- The hybrid system presented different efficiencies stages and as a result there are electric and heat losses (unrecoverable energy), associated with electrical efficiency and total fuel cell efficiency, respectively. In this case, the fuel cell performance is 42% higher than the electric efficiency.

- As a result, the PV-H2-SOFC system allows supply a higher electric demand and adds thermal consumption as hot water. Furthermore, it has cogeneration benefits, such as the environmental impact due to hydrogen obtained from PV panels, which is used in the fuel cell. Also, in this process, there is heat recovery, so it is a closed energy cycle.

- Despite that the integration of fuel cell into PV system showed an economic disadvantage, there is financial retribution for the sale of the surplus energy, improving the energy cost balance. Besides, the system can supply a higher demand for the same cost, considering, for example, thermal energy consumption.

REFERENCES

[1] G. Bourne, P. Scrock, and A. Stock. “Powering progress: States renewable energy race,” 16 Oct 2018. [Online]. Available: https://www.climatecouncil.org.au/resources/states-renewable-energy/. [Accessed 3 Jun 2019].

[2] L. Brailsford, A. Stock, G. Bourne, and P. Stock. “Powering progress: States renewable energy race,” Climate Council of Australia, 2018.

[3] e. a. t. (Australian Government Department of Resources, G. Australia and A. B. o. A. a. R. Economics, “Australian energy resource assessment,” 2010. [Online]. Available: https://d28rz98at9flks.cloudfront.net/70142/70142_complete.pdf. [Accessed 4 June 2019].

[4] S. Bruce, M. Temminghoff, J. Hayward, E. Schmidt, C. Munnings, D. Palfreyman, and P. Hartley. “National Hydrogen Roadmap: Pathways to an economically sustainable hydrogen industry in Australia,” CSIRO, 2018.

[5] Australian Energy Regulator. “Energy made easy- Understand and compare your home energy usage,” Australian Government, 24 April 2019. [Online]. Available: https://www.energymadeeasy.gov.au/benchmark. [Accessed 16 May 2019].

[6] European Commission. “Photovoltaic geographical information system,” 21 Sept 2017. [Online]. Available: http://re.jrc.ec.europa.eu/pvg_tools/en/tools.html. [Accessed 19 May 2019].

[7] S. Allende. “Energy analysis of a solid oxide fuel cell (Sofc) operated by PV system in the residential sector, in Highland,” M.A. thesis, GRIN Verlag, Munich, 2018.

[8] F. Brihmat, and S. Mekhtoub, “PV cell temperature/ PV power output relationships homer methodology calculation,” National Superior Polytechnic School, Algeria, 2014.

[9] M. Jeffrey, I. Kelly, T. Muneer, and I. Smith. “Evaluation of Solar Modelling Techniques Through Experiment on a 627 kWp Photovoltaic,” Journal of Renewable and Sustainable Energy, vol. 7, no. 3, 2105

[10] Advanced Solar Photonics. “ASP-400GSM - smart moduletm series - high efficiency frameless monocrystalline solar modules,” 2012. [Online]. Available: https://www.enfsolar.com/Product/pdf/Crystalline/50bd9203a2fc0.pdf. . [Accessed 20 May 2019].

[11] T. Muneer, R. Milligan, I. Smith, A. Doyle, M. Pozuelo, and M. Knez. “Energetic, environmental and economic performance of electric,” Edinburgh, Transportation Research Part D: Transport and Environment, 2015, pp. 40-61.

[12] A. Kabza. “Fuel cell formulary,” 9 Nov 2016. [Online]. Available: http://www.pemfc.de/FCF_A4.pdf. [Accessed 21st May 2019].

[13] D. Steward. “National renewable energy laboratory,” FCPower model simulation, 2013. [Online]. Available: https://www.nrel.gov/hydrogen/fuel-cell-power-model.html. [Accessed 5 May 2019].

[14] A. El-Maaty. “Modelling and Simulation of a

Photovoltaic Fuel Cell Hybrid System," PhD. thesis, University of Kassel , Kassel, 2005.

[15] Battelle Memorial Institute, "Manufacturing cost analysis of 100 and 250 kW fuel cell systems for primary power and combined heat and power applications," U.S. Department of Energy, 2016.

[16] T. Yuan, Q. Duan, X. Chen, X. Yuan, W. Cao, J. Hu, and Q. Zhu. "Coordinated control of a wind-Methanol-Fuel cell system with hydrogen storage," MDPI, Basel, 2017.

[17] S. Downes. "Perth electricity prices compared," 7 Jan 2019. [Online]. Available: https://www.canstarblue.com.au/electricity/perth-electricity-prices/. [Accessed 1 Aug 2019].

[18] D. Goos. "Feasibility Study of a Solar Charging Facility for Electric Vehicles in Munich," M.A. thesis, Edinburgh, 2015.

[19] L. Parry. "Greener Kirkcaldy," 2015. [Online]. Available: http://www.greenerkirkcaldy.org.uk/how-much-energy-are-your-home-appliances-using/. [Accessed 13 May 2018].

[20] ACS Chemistry for life. "The energy efficiency of heating water," [Online]. Available: http://highschoolenergy.acs.org/content/hsef/en/how-can-energy-change/energy-efficiency-of-heating-water.html. [Accessed 17 June 2018].

[21] E. Gago, S. Etxebarria, Y. Tham, Y. Aldali, and T. Muneer. "Inter-relationship between mean-daily irradiation and temperature, and decomposition models for hourly irradiation and temperature," International Journal of Low-Carbon Technologies, vol. 6, no. 1, pp. 22-37, 2010.

[22] A. Ganguly, D. Misra, and S. Ghosh. "Modeling and analysis of solar photovoltaic-electrolyzer-fuel cell hybrid power system integrated with a floriculture greenhouse," Department of Mechanical Engineering, Bengal Engineering & Science University, Shibpur,, West Bengal, 2010.

[23] K. Ro, and S. Rahman, "Battery or Fuel Cell Support for an Autonomous Photovoltaic Power System," Renewable energy, vol. 13, no. 2, pp. 203-213.

[24] J. Guan, N. Minh, B. Ramamurthi, J. Ruud, J.-K. Hong and P. Riley. "High Performance Flexible Reversible Solid Oxide Fuel Cell," United States Department of Energy , Torrance, 2004.

[25] W. Saeed, and G. Warkozek, "Modeling and analysis of renewable PEM fuel cell system," International Conference on Technologies and Materials for Renewable Energy, Environment and sustainability, pp. 87-101, 2015.

[26] G. Wu, K. Y.Lee, L. Sun, and Y. Xue. "Coordinated fuzzy logic control strategy for hybrid PV array with fuel-cell and ultra-capacitor in a Microgrid," Department of Electrical and Computer Engineering, Bejing, 2017.

[27] M. Hosseini, I. Dincer, and M. Rosen. "Investigation of renewable energy-Based integrated system for baseload power generation", Progress in Sustainable Energy Technologies:, Generating Renewable Energy, pp. 21-46, 2014.

[28] M. M. Elamari. "Optimisation of Photovoltaic Powered Electrolysis for Hydrogen Production for a Remote Area in Libya," PhD, University of Manchester, Manchester, 2011.

[29] Business Juice. "Business energy prices by region," 2017. [Online]. Available: https://www.businessjuice.co.uk/energy-guides/energy-prices-by-region/. [Accessed 24 July 2018].

[30] N. Hill, and R. Watson. "2016 government GHG conversion," Department of Business Energy & Industrial Strategy (BEIS), London, 2016.

[31] D. Steward, M. Penev, G. S. Becker, and W. Becker. "Modeling electricity, heat, and hydrogen generation from fuel cell-based distributed energy systems," National Renewable Energy Laboratory, 2013.

[32] Clean Energy Council. “Clean energy Australia,” 9 April 2018. [Online]. Available: https://assets.cleanenergycouncil.org.au/documents/resources/reports/clean-energy-australia/clean-energy-australia-report-2018.pdf. [Accessed 1st March 2019].

[33] J. Lagorse, D. Paire, and A. Miraoui. “Sizing optimization of a stand-alone street lighting system powered by a hybrid system using fuel cell, PV and battery,” Renewable Energy, vol. 34 , no. 3, pp. 683-691, 2009.

[34] M. Jamshidi, and A. Askarzadeh. “Techno-economic analysis and size optimization of an off-grid hybrid photovoltaic, fuel cell and diesel generator system,” Sustainable Cities and Society, vol. 4, pp. 310-320, 201.

[35] M. Qandil, R. Amano, and A. Abbas, “A stand-alone hybrid photovoltaic, Fuel Cell and Battery System,” Proc. of the ASME 2018 12th International Conference on Energy Sustainability, pp. 24-28, 2018.

[36] H. Rezkab, E. Taha, M. Al-Dhaifallahe, M.Obaidcf, A. Hashema, M.El-Sayedb, M. Ali, and G.Olabi. “Fuel cell as an effective energy storage in reverse osmosis desalination plant powered by photovoltaic system,” Energy, vol. 175, pp. 423-433, 2019.

Journal of Renewable Energy and Sustainable Development (RESD) Volume 5, Issue 2, December 2019 - ISSN 2356-8569
http://dx.doi.org/10.21622/RESD.2019.05.2.068

COMPREHENSIVE REVIEW OF PUMP AS TURBINE (PAT)

Abdulbasit Nasir Jemal[1], Misrak Girma Haile[2]
Department of Mechanical Engineering, Addis Ababa Science and Technology University, Addis Ababa, Ethiopia.
abdulbasitnasir@ymail.com[1], misrakmgh@gmail.com[2]

***Abstract* -** The turbine is a heart of power generation in a hydro-electric power system. A variety of different turbines are available for that purpose. The common types of Hydraulic turbines are; Pelton, cross flow, Francis, Kaplan, and propeller turbine. However, using conventional turbines for low head and flow rate (i.e. micro hydropower) applications are not economically feasible. A low-cost alternative is to use the pump as a turbine. In this paper, existing Peer-reviewed articles from (Scopus, google scholar, umbrella, etc.) that are directly related to pump running as a turbine are collected and reviewed. Theoretical, numerical, and experimental investigations are considered. Performance improvement techniques for PAT are summarized and research gaps in related works are identified.

***Keywords* -** Turbines, Pumps, Review, Pump as Turbine, PAT.

List of Abbreviations and symbols -

BEP	Best Efficiency Point
b2	impeller inlet width (mm)
b3	volute outlet width (mm)
C	absolute velocity of the fluid
CFD	Computational Fluid Dynamics
C_H	coefficient of head
C_Q	coefficient of flow rate
D1	impeller outlet diameter (mm)
D2	impeller inlet diameter (mm)
D3	volute base circle diameter (mm)
D4	volute inlet diameter (mm)
g	gravitational acceleration (m/s2)
H_{bep}	head at best efficiency point (m)
H_p	pump head (m)
H_p''	theoretical head (m)
I	turbulence intensity
ICEM	Integrated Computer Engineering and Manufacturing
k	turbulent kinetic energy (J/kg)
N-S	Navier-stock
n_{SP}	specific speed of pump (m, m3/s)
n_{ST}	specific speed of turbine (m, m3/s)
PAT	Pump as Turbine
PDE	Partial Differential Equation
PISO	Pressure-Implicit with Splitting of Operators
P_h	hydraulic power (W)
P_m	mechanical power (W)
Q_{bep}	flow rate at best efficiency point (L/s)
Q_p	pump flow rate (L/s)
rpm	revolution per minute
Re	Reynold's number
RNG	Re-normalization group
SST	shear stress transport
U	peripheral/tangential velocity of wheel (m/s)
V	relative velocity of fluid (m/s)
y+	y plus
Z	number of blades
α	flow angle (0)
β1	blade outlet angle (0)
β2	blade inlet angle (0)
ηbep	efficiency at best efficiency point
η_p	pump efficiency (%)
µ	slip factor for pump operation
λ	slip factor for turbine operation
ε	turbulence dissipation
ω	specific dissipation rate (rad/s)
ϕ	discharge number
Ψ	head number
π	power number

I. INTRODUCTION

The turbine is a heart of power generation in a hydro-electric system. A variety of different turbines are available for that purpose. However, using conventional turbines for low head and flow rate (micro hydro power) applications is not economically feasible [1]. A low-cost alternative is to use a Pump as Turbine (PAT).

Pumps are widely used for irrigation, industrial and domestic applications, transportation of liquid, industrial processes, as well as heating and cooling systems [2]. Flow directions of the pump are shown in Fig. 1.

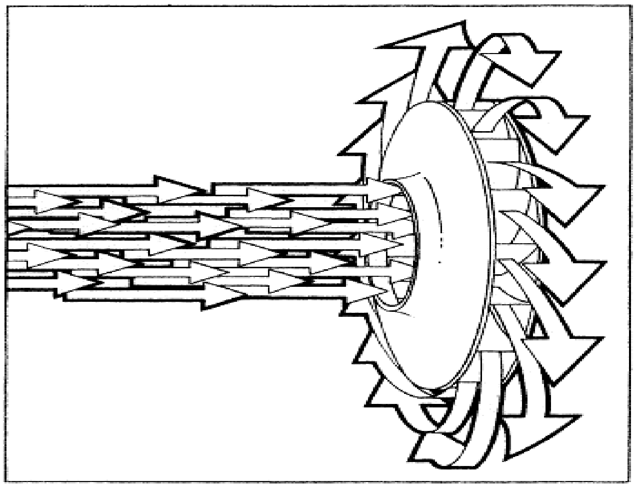

Fig .1 Flow direction of the pump [2].

In addition to the basic functions, pumps can be used to generate electricity when operating in a reverse way. The basic hydraulic theory of both pump and turbine modes to be is the same, Fig. 2. However, the behavior of real fluid flow including friction and turbulence result is different [3].

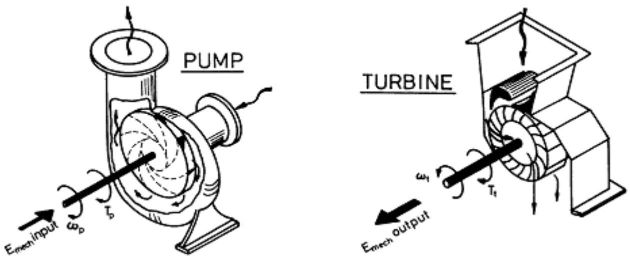

Fig .2 Flow direction in pump and turbine modes [4].

PAT can be applied to micro-hydropower plants as well as water supply piping and distribution systems [5-9], reverse osmosis systems [10], pressure reducing system [11, 12], energy recovery in irrigation networks and industries [13-22].

Pumps have various advantages compared to turbines, such as availability, proven technology, low initial installation and maintenance cost, available for a wide range of heads, and flows [1, 7]. Pump impellers have no significant disadvantages in turbine mode, but the efficiency coefficient of a pump in turbine operation is lower [16]. The pump manufacturers do not provide characteristic curves of their pumps working as turbines. This makes it difficult to select a suitable pump to run as a turbine for a specific application [23].

In this paper, existing peer-reviewed articles from (Scopus, google scholar, umbrella, etc.), that are directly related to pump running as a turbine, are collected and reviewed. Peer-reviewed articles other than review papers are considered. Theoretical, numerical, and experimental investigations are studied. Performance improvement techniques for PAT are summarized and research gaps in related works are identified.

Pump manufacturers only supply pump mode performance curves and that makes it difficult to predict the performance of the pump working as a turbine. Three main ways of conducting researches on the pump running as a turbine are: analytical/theoretical method, the numerical/computational method, and the experimental method.

II. THEORETICAL INVESTIGATION OF PAT

A theoretical investigation is the study of fluid flow problems analytically, using partial differential equations without any approximations. Many attempts have been made to predict pump in turbine mode performance theoretically. A mathematical model was applied to investigate the installation of PAT, by solving the system of partial differential equations into ordinary differential equations [7].

It was found that pump impellers have no significant disadvantages in turbine mode and the efficiency coefficient of a pump in turbine operation is hardly lower (in some cases even higher) than in pump operation [16]. The efficiency at the BEP in turbine mode corresponds approximately to the efficiency coefficient in pump mode.

$$\eta bep_T = \eta bep_P \pm 0.02 \quad (1)$$

If the rotational speeds are the same for both modes, there are equal and opposite heavy line velocities for pump mode and turbine modes based on the infinite-blade theory. Consequently, Euler head in pump and turbine mode are the same [19,24].

$$H_{Euler} = \frac{u_1 v_{u1} - u_2 v_{u2}}{g} \quad (2)$$

Where V_{u1} and V_{u2} represent the peripheral component of velocity at the high-pressure side and low-pressure side, respectively.

In equation (2), v_{u2} is negligibly small in general and, as a result, the Euler head can be as

$$H_{P\ Euler} = \frac{u_1 v_{u1}}{g} = H_{T\ Euler} \quad (3)$$

Due to slip of finite blade number, pump and turbine theoretical head is given by:

$$H_p^{"} = \mu H_{p\ Euler} \quad (4)$$

$$H_t^{"} = H_{t\ Euler}/\lambda \quad (5)$$

Where μ is a slip factor for pump operation μ < 1, λ is a slip factor for turbine operation. The slip factor for reverse mode is approximately equal to 1.0 [4].

From the fundamentals of energy transfer in turbines, the output mechanical shaft power and Euler turbine head can be represented by [25]:

$$P = \rho g Q H_t - P_{mech} - P_{leak} \quad (6)$$

$$H_t = \sigma H_{Euler} \quad (7)$$

$$H_{Euler} = \frac{(U_2 C_{u2} - U_1 C_{u1})}{g} = \frac{(U_2 C_{m2} cot\alpha_2 - U_1(U_1 - C_{m1} cot\beta_1))}{g} = \frac{(U_2 \left(\frac{Q}{A_2}\right) cot\alpha_2 - U_1\left(U_1 - \left(\frac{Q}{A_1}\right) cot\beta_1\right))}{g} \quad (8)$$

PAT's P-Q curve is in inverse proportion to the inlet area A_2. PAT's required pressure head can be represented as the sum of the theoretical head and the losses. PAT's hydraulic efficiency can be represented by:

$$\eta_h = \frac{H_t}{H_t + h_{total}} \quad (9)$$

Both theoretical head and total hydraulic loss increase with the increase of the blade thickness.

In the study of S. Barbarelli et al. [26], a statistical method combined with a numerical model for selecting a pump running as turbine in micro-hydro plants is applied. The information of the site (flowrate and head) allow calculating two coefficients, C_Q and C_H, respectively.

For searching of energy conversion characteristics of PAT in detail, theoretical analysis and empirical prediction can only outline the energy conversion characteristics in the macroscopic point of view [27].

By considering the PAT's flow, i.e. the reverse of pump, the theoretical head transferred from the fluid to the runner is smaller than actual head HT between the inlet and exhaust nozzles because of the hydraulic losses Z [28]. Because of power losses, the power PT available at the coupling of the turbine is smaller than the hydraulic power $\rho g H Q$. The PAT's overall efficiency η_T is:

$$\eta_T = \frac{P}{\rho g H Q} \quad (10)$$

The basic parameters of pump and turbine mode are specific and deal with (i) geometric characteristics; (ii) flow and geometrical angles, and (iii) hydraulic and power losses. These parameters may be known from pump geometry or can be estimated through an optimization procedure [28].

The effect of variable guide vane numbers on the performance of pump as turbine was analyzed theoretically, having the turbulence kinetic energy under variable working conditions. The asymmetry of the volute and rotor-stator interaction causes turbulence kinetic energy concentration to appear in pump as turbine. Theoretically, the turbulence kinetic energy equals half of the product of turbulent velocity fluctuation variance and fluid mass, which generally is expressed by the physical quantity k and can be calculated through the turbulence intensity I [29].

$$k = \frac{3}{2}(uI)^2 \quad (11)$$

$$I = 0.16 Re^{\frac{-1}{8}} \quad (12)$$

Many attempts have been made to predict turbine mode performance by using analytical/theoretical model but the percentage of deviation is comparatively large compared to the actual performance. It can be concluded that the theoretical method is used to study flow problems with a few variables, while it is difficult to analyze pumps running as a turbine.

III. NUMERICAL INVESTIGATION OF PAT

A numerical investigation is the study of fluid dynamics problem using computer software, in this case approximating partial differential equations into system algebraic equitation. Computational Fluid Dynamics (CFD) is an active design tool for predicting the performance of centrifugal pumps running in turbine mode.

Flow Conditions for PATs Operating in Parallel was performed using the CFD model [1]. The k- ε turbulent model is adopted, the domain has 713,954 cells. Variables, such as mass flow rate, outlet pressure, and rotational speed, and rotating zone are specified in Fig. (3). When the flow is different from the normal rated conditions, two PATs in parallel can better cover it.

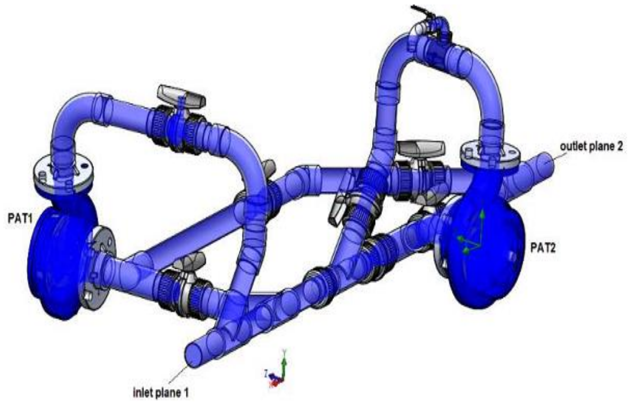

Fig .3 PAT's system set-up [1].

The behavior of the pressure distribution when PAT installing in a water network was analyzed [11]. The PAT model was built in SolidWorks, then simulated by using CFD, the boundary conditions are specified and the number of elements is about 100,000. The global variables are simulated in the CFD model and used to evaluate the overall PAT characteristics. Results of numerical and experimental values do relatively not agree.

The pressure fluctuation characteristic of the hydraulic turbine at a single rotational speed with guide vane was analyzed [13]. Unlike others in this work, the PISO algorithm is adopted to solve the Navier-Stokes equations. RNG k-ε turbulence model was used for this specific purpose. The grid independence is verified. the final grid number is 1,042,502. In the impeller blade region, the pressure fluctuation in the pressure surface is lighter than that of the suction surface.

The slip phenomenon was investigated and the effective value of slip factors for both direct and reverse modes is obtained. Pump and turbine head impeller can be predicted by computational fluid dynamics [19].

$$H_p = \frac{H_p}{\eta_{hp}} \qquad (13)$$

$$H_t = H_t * \eta_{ht} \qquad (14)$$

ANSYS-CFX was selected for the solution. A grid sensitivity analysis was performed. The final elements number of the fluid volume was 4,154,084. Testing different turbulence models, and RNG k- ε model confirms a good accuracy in the performance prediction of PAT. At BEP the effective value of slip is 0.28 for pump and 0.24 for turbine mode. Pump and PAT can be related

$$\frac{H_t}{H_p} = \frac{1-s_t}{1-s_p}\frac{1}{\eta_{ht}\eta_{hp}} \qquad (15)$$

A Performance Prediction Method for three different Pumps as Turbines using a computational fluid dynamic modeling approach was presented [23]. Results have been first confirmed in pumping mode using data supplied by pump manufacturers. Then, the model results have been compared to experimental data for PAT. The analyzed pumps have three different specific speeds. The main characteristics are summarized in Table (1). From the CFD model results, the specific head, capacity, power, and efficiency have been evaluated and the best efficiency point of all the analyzed pumps was found.

Table 1 Characteristics of Different Pumps [23]

	Impeller diameter (mm)	Delivery outlet diameter (mm)	$H_{bep}(m)$	$Q_{bep}(m^3/h)$
$(N_s\ 37.6)$	190	80	39	148
$(N_s\ 20.5)$	200	70	60	45.4
$(N_s\ 64.0)$	120	80	3.9	54

For all cases, the maximum value is lower than the pump mode value. For low specific speed pumps, this maximum value is roughly equal to the pump mode, while for high specific speed pumps, it is different. Model results for Pump 1 at 2900 rpm are shown in Fig. 4 and the pressure distribution at the BEP in the 0–9 bar pressure range is presented.

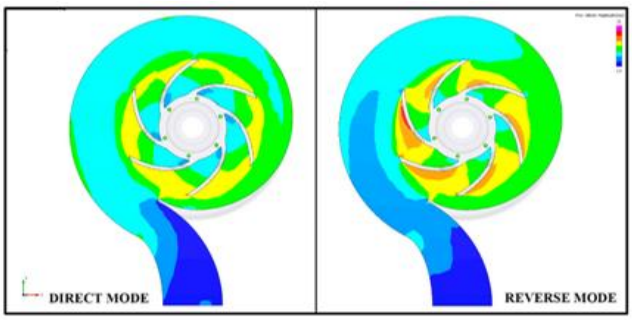

Fig .4 Pressure distribution of model results for pump 1 (Ns = 37.6) at 2900 rpm [23].

It is clear that maximum pressure is applied in reverse mode. This indicates that blade modification is required when using the pump as a turbine.

A single-stage centrifugal pump was selected for energy conversion characteristic of pump as turbine [27]. The centrifugal pump design parameters are: flow rate Q = 12.5 m^3/h, head H= 30.7 m, rotating speed n = 2900 rev/min, specific speed ns = 48, and the shape of the blade is cylindrical. The impeller is divided into six regions as shown in Fig. (5) by the radius.

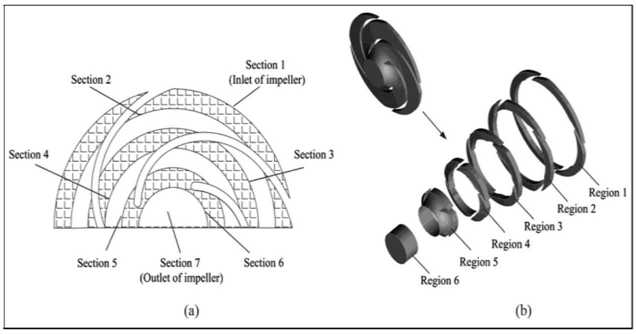

Fig .5 Schematic diagram of the impeller division of the PAT [27].

ICEM was used to generate a structured hexahedral mesh for each part. The grid number is about 1.1 million. The ANSYS-FLUENT was selected to calculate PDE. The standard k–e turbulence model was chosen. The results show that the front and middle part of the impeller i.e. (0.6–1.0) D2) are significant parts for energy conversion; in the rear area of the impeller. Thus, the PAT blades need to be optimized to improve the performance, especially in the impeller blade rear area.

Turbulence model has its own influence on the accuracy of the result. In the numerical method, a variety of turbulence models are available, among them RNG k-ε [13, 19], standard k-ω [22], and standard k- ε [1, 6, 11, 23, 25, 27, 29 and 30] are used to predict the effects of turbulence on the system. Because of the irregularity shape of impeller unstructured mesh found to be the best one, but the result of review indicates, many researchers used structured mesh.

Pressure fluctuations are very vital characteristics in pump turbine's operation. 3D numerical simulations using SST k-ω turbulence model was carried out to predict the pressure fluctuations distribution in a prototype pump-turbine at pump mode [31]. Three operating points with different flow rates and different guide vanes openings were simulated. The numerical results show how pressure fluctuations at blade passing frequency and its harmonics vary along with the whole flow path direction, as well as along the circumferential direction.

A complete numerical detail for a selection of centrifugal pump as turbine with a rotational speed of 2880rpm for micro-hydro power plants was provided [32]. The maximum power output is 17.78 KW. The BEP of centrifugal pump operated in pump mode was observed as 70% of that to turbine mode was 35.45%. It was clear that the pump relatively operated as a turbine is with lower efficiency. The future work focuses on the further development of PAT performance.

Hydraulic design and optimization of a modular pump-turbine runner were performed [33]. A mesh discretization study was performed and found that convergence was reached around a nine million cell mesh. The runner's performance was characterized in both the pump and turbine modes for its designed working conditions for both the initial and optimized design.

Numerical simulations were done to predict the distribution of pressure fluctuations with different numbers of runner blades in turbine mode using the k-ω turbulence model [34]. The two factors that influence the distribution of pressure fluctuations found to be the flow rate and a number of blades, especially at blade passing frequency along the circumferential direction. The power loss and radial force characteristics of the pump as a hydraulic turbine under gas-liquid two-phase condition was studied [35]. Based on the N-S equation and standard k-e turbulence model, computational fluid dynamics technology was used to simulate the flow field in a hydraulic turbine. The result illustrates that the gas content has a serious effect on PAT performance. Under the two-phase condition, the fluid velocity distribution in turbine mode is uneven, and the power loss is not uniform enough when the gas content is lower.

Mesh refine [1, 6, 11, 19, 22, 23 and 25] especially at the boundary and the inlet of the pipe is used to:

- save memory capacity
- decrease computational time

In all cases, the value of the numerical result is higher than the experimental one. This indicates that numerical methodology is not enough to determine the exact solution of pump running as a turbine.

IV. EXPERIMENTAL INVESTIGATION OF PAT

The experimental investigation is the study of fluid flow problem using physical laboratory. Knapp (1941) published the complete pump characteristics for a few pump designs based on experimental investigations [36].

Two equal PATs working in parallel and single-mode were performed [1]. Several experimental tests at a different flow rate (200 to 1150) were carried out for the two configurations by regulating the flow rate. During each test, the data were recorded. The performance in parallel design conditions illustrates a peak efficiency with less shock losses within the impeller.

The hydraulic facility, composed of one closed pipe, an air-vessel tank (allows to regulate the flow and pressure in order to reach the steady flow conditions) a recirculating pump, an open free surface tank, ball valves, an electromagnetic flowmeter, two pressure transducers were used to determine the behavior of the pressure distribution along the PAT [11].

The pressure fluctuation characteristic of a hydraulic turbine with guide vane using the test bench Fig. 6 was studied [13], with different flow rate. The pressure fluctuation is also different, the greater the flow rate, the more serious the pressure fluctuation.

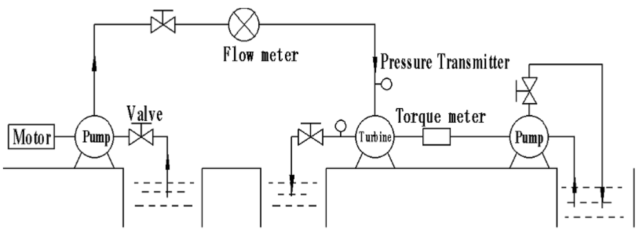

Fig .6 Test bench for hydraulic turbine [13]

Three centrifugal pumps with different heads and flow rates have been modeled and tested in the test bench [13], unitless parameters are calculated.

Head number $\Psi = \frac{gh}{n^2 D^2}$ (16)

discharge number $\phi = \frac{Q}{nD^3}$ (17)

power number $\pi = \frac{p}{\rho n^3 D^5}$ (18)

efficiency $\eta = \frac{P}{\rho Q H}$ (19)

Experimental investigations and laboratory measurements on the hydraulic machine are conducted at a turbine test rig to validate the theoretical work that is used to predict the behavior of a centrifugal stainless-steel pump in turbine operation [16].

A centrifugal multistage end-suction pump chosen for experimental investigation [17]. The test rig consists of the pump with a synchronous motor, two pressure transducers, a magnetic flow meter, a watt meter, and an optical speedometer. The focus of the study was comparing direct and indirect water supply a network and direct pumping found to be considered to be more efficient than indirect pumping.

Equation 16 through 19 used to determine the characteristics of the pump running as a turbine. A laboratory model of PAT test rig was used to conduct research on energy conversion characteristics of the pump as a turbine [27]. The main equipment composed of an electric motor, a feed pump, a control valve, an electromagnetic flow meter, a differential pressure transducer, a PAT, a torque meter, and an energy dissipation pump.

The characteristics of energy transformation, especially within impeller, plays significant roles for further optimum design of the pump as turbine, the area of (0.6–1.0) D2) are important parts for energy conversion; in the rear area of the impeller, this at least shows that the PAT blades need to be optimized to improve the performance, especially in the impeller blade rear area.

The feasibility study of using pumps in turbine mode in small hydroelectric stations was presented [37]. To regulate the power applying variations in the turning speed of the turbine-generator set.

The study of A. Carravetta et al. [38] affinity law for the evaluation of the behavior of a single machine under variable speed. The study shows that the use of performance curves calculated using affinity law and Suter parameters produces a limited error in the evaluation of the head drop, granting the satisfaction of the correct hydraulic constraint (pressure level within the network). Meanwhile, the error in terms of mechanical efficiency is greater but still acceptable in a limited range of velocity difference between a prototype and simulated machine.

An end suction centrifugal pump with a specific speed of 15.36 (m, m3/s) was tested experimentally, to determine the performance characteristic of the pump in reverse mode. The result showed that a centrifugal pump can satisfactorily be operated as a turbine without any mechanical problems. The best efficiency point (BEP) for PAT was found to be lower than BEP in pump mode [39].

There are some variations between numerical and experimental results in the case of PAT. As recommended by many researchers the variation can be minimized through development by using a fine grid and introducing appropriate turbulence models.

The solution of the pump running as a turbine highly depends on different conditions like flow rate, head, impeller diameter, and rotational speed. Tasting and measuring PAT output with various parameters as done by many investigators is very important to predict a relatively more accurate solution.

V. MODIFICATION IN PAT

The result of the study shows the efficiency of PAT is 12.4 % [12], 4% [21], 34.55% [32], 19 % [39] lower than direct pump mode. The result of all investigations shows that the pump has low efficiency in turbine mode, geometric modification is required to improve the efficiency pump working as a turbine.

The influence of the different number of blades (10-13) with guide vane on the performance of PAT was investigated numerically and experimentally [22]. To perform the numerical simulation, applying ANSYS CFX and k-ω the turbulence model was used. Meshing is performed by ICEM. The grid independence is verified. The total number of grids is 15.287 million.

The PAT test bench consists of a model PAT, an overrunning clutch, an electric motor, a centrifugal pump, throttle valves, and bypass valves, and a pool is used to validate relationship curves among the head, efficiency, power, and flow rate of the PAT, which are drawn and compared with the simulation result. Results show that when the number of blades is 10 at the same flow rate, the highest efficiency is achieved and the internal flow becomes stable.

PAT covering different specific speeds was designed to explore the effects of blade thickness on the performance [25]. Numerical and experimental methodologies are applied. ICEM-CFD was used to generate the structured hexahedral grid for the components. A grid-independent test was performed. The final mesh number is over 1 million and the standard k-ε model was applied. After modification, a new impeller was manufactured and verified in the test rig. The efficiency decreases with increasing blade thickness. Using the thinner blades with sufficient strength to obtain higher efficiency was recommended. Based on the founding of research appropriate material selection is an important factor for the improvement of PAT.

Energy conversion characteristic of pump as turbine by considering a single-stage and single-suction centrifugal pump running in the reverse model as the turbine was selected [27]. The centrifugal pump design parameters are: flow rate Q = 12.5 m^3/h, head H= 30.7 m, rotating speed n = 2900 rev/min, specific speed ns = 48, and the shape of the blade is cylindrical. The result of the study shows that PAT blades need optimization to enhance the performance, especially in the impeller blade rear area.

Blade profile optimization by using a numerical approach was performed [30]. Coordinate values of the control point 1-8 in Fig. 7 were selected as the optimization design variables. The control point 9 remains unchanged.

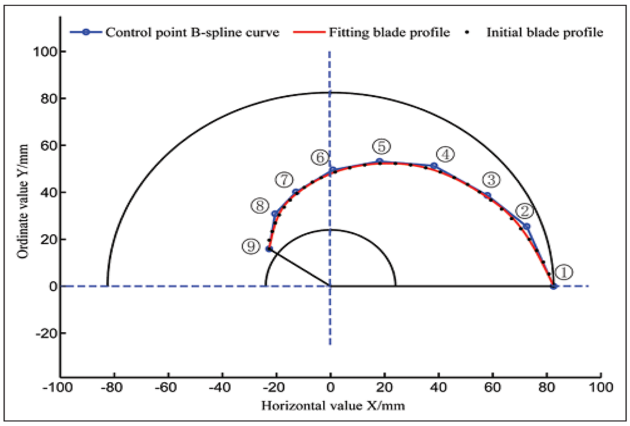

Fig .7 Blade parameterization (30).

The ANSYS-FLUENT software is used to calculate the selected model in the numerical method. N-S equations to describe the inner flow of the PAT, the standard k–e turbulence model is used. ICEM was used to generate the structured grid of computational domain. The final mesh number is 1,178,560.

The result shows that the efficiency of the optimized pump as turbine under the optimum operating condition increased by 2.91%. Through optimization of the blade, the hydraulic loss in the impeller decreased, the hydraulic loss in the volute and outlet pipe has a certain increase, whereas the total hydraulic loss decreased. Further investigation is required to control the hydraulic loss in the volute and outlet pipe.

One original impeller and three modified impellers of an industrial centrifugal pump with a specific speed of 23.5 m, m3 /s were tested numerically and experimentally. In this work, the shape of blades was redesigned to reach a higher efficiency in turbine mode using a gradient-based optimization algorithm coupled by a 3D Navier–stokes flow solver. Also, another modification technique was done by rounding the leading edges of blades and hub/shroud interface in turbine mode [40]. The result of the study shows modifications on the impeller lead to achieving maximum efficiency in reverse mode.

A comparison between centrifugal impeller pumps mode [41] and turbine mode [42], with and without splitter blades in terms of suction performance, is presented by experimental tests and numerical analyses. The efficiency of PAT is improved when splitter blades are added to impeller flow passage.

Multi-objective optimization to improve the hydrodynamic performance of a counter-rotating type pump-turbine operated in pump and turbine modes was illustrated [43]. The inlet and outlet blade angles of impellers/runners with four blades, which were extracted through a sensitivity test, were optimized using a hybrid multi-objective genetic algorithm with a surrogate model based on Latin hypercube sampling. Three-dimensional steady incompressible Reynolds-averaged Navier-stokes equations with the shear stress transport turbulence model were discretized via finite volume approximations and solved on a hexahedral grid to analyze the flow in the pump-turbine domain. For the major hydrodynamic performance parameters, the pump and turbine efficiencies were considered as the objective functions. The result shows that the arbitrarily selected optimal designs in the Pareto-optimal solutions were increased as compared with the reference value.

Many researchers have reported that the efficiency of pump in turbine mode can be improved by simple modification such as rounding impeller tips, installation of splitter blades, reducing impeller thickness, increasing number of blades, applying of guide vane, and optimizing blade profile . Table 2 summarizes the outcome of the modifications different researchers made.

Table 2 Summary of modification result proposed by different researchers.

Author	Shi et al. [22]	Yang et al. [25]	Feng Xia Shi et al. [29]	S. Miao et al. [30]	S. Derakhshan et al. [40]		P. Singh and F. Nestmann [44]
Method	Number of blades	Blade thickness	Guide vane number	Blade profile optimization	Rounding of inlet	Optimization	Impeller rounding
Rise in efficiency (η%)	≈1.75	≈1.6	≈2	≈2.91	≈5.5	≈2.75	≈2

Among the various techniques attempted by different investigators for performance improvement of pump as turbine, rounding of impeller inlet and blade profile optimization is found to be the most promising technique. Testing of more than one modification techniques per system is important to further improvement.

VI. RESEARCH GAPS IN RELATED LITERATURE

When the pump is operating in the turbine mode, the direction of flow is reversed; therefore, the pattern of loss distribution is not the same as in the pump mode. To improve performance, one of the important factors is to identify the causes of losses that may occur in turbine mode. Many researchers have studied performance improvement of PAT focusing on shock loss, while other losses such as diffusion and hydraulic losses should be considered when using pump as turbine.

Guide vane is an important part of a turbine, but centrifugal pumps have no guide vane. An extra row of fixed blades called inlet guide vane are required to direct the water at the correct angle onto the PAT blade; therefore, testing and using different guide vane angle are important to improve the efficiency of the system.

There is a need for studies that focus on the multi-stage multi-flow pumps to increase the power output from pump as turbine (PAT). Furthermore, a comparative study is needed to provide information on the various turbulence models then finding out the best one.

The velocity triangle is one of the fundamental tools to analyse turbomachinery problems. After each modification, the velocity triangle of the modified blade should be specified.

Cavitation is caused by local vaporization of the liquid. It usually occurs in hydraulic machines and it is a cause of different potential problems. Optimum design is required to avoid the effect of Cavitation.

VII. CONCLUSION

In various parts of this review paper, it has been recognized that extensive studies have been carried out on pump as turbine. From the entire study, it can be concluded that Commercial centrifugal pump, i.e. PAT, will provide an attractive alternative for power generation in off-grid areas. The limitations of PAT can be further reduced by selecting a proper pump for a specific site. The characteristics of the pump running as a turbine can be predicted by a theoretical, numerical, and experimental approaches. The efficiency can be increased by using various modification techniques. Among the various techniques attempted by different researchers is rounding of impeller inlet and blade profile optimization, which were found to be the most promising techniques.

For future research, in addition to introducing new modifications, a study on the importance of applying existing techniques should be carried out.

REFERENCES

[1] M. Simão, M. Pérez-Sánchez, A. Carravetta, and Helena M. Ramos, "Flow conditions for PATs operating in parallel: Experimental and numerical analyses," Energies, vol. 12, pp 901, 2019. doi:10.3390/en12050901

[2] Val S. Lobanoff, and Robert R. Ross, "Centrifugal Pumps Design & Application". 2nd ed. United States of America: Gulf Publishing Company, 1992.

[3] S. Derakhshan, and A. Nourbakhsh, "Theoretical, numerical and experimental investigation of centrifugal pumps in reverse operation," Elsevier, Experimental Thermal and Fluid Science, vol. 32, pp. 1620–1627, 2008. doi:10.1016/j.expthermflusci.2008.05.004

[4] J. Chapallaz , P. Eichenberger , and G. Fischer, "Manual on Pumps Used as Turbines" MHPG Series; vol. 11; Germany, Friedr. Vieweg & SohnVerlagsgesellschaftmbH, 1992.

[5] A. Carravetta, G. Del Giudice, O. Fecarotta, and H. M. Ramos, "Pump as Turbine (PAT) design in water distribution network by system effectiveness," Water, vol. 5, pp. 1211-1225, 2013. doi:10.3390/w5031211

[6] J. B. Bogdanovic-Jovanovic, D. R. Milenkovic, D. M. Svrkota , B.Bogdanovic, and Z. T. Spasic, "Pumps used as turbines power recovery, energy efficiency, CFD analysis," Thermal Science, vol. 18, pp. 1029-1040, 2014. doi:10.2298/TSCI1403029B

[7] M. De Marchis, B. Milici, R. Volpe, and A. Messineo, "Energy saving in water distribution network through pump as turbine generators: Economical and environmental analysis," Energies, vol. 9, pp. 877, 2016. doi:10.3390/en9110877

[8] J. Kim, B. Cho, S. Kim, J. Kim, J. Suh, Y. Choi, T. Kanemoto, J. Kim, "Design technique to improve the energy efficiency of a counter rotating type pump-turbine," Renewable Energy, vol. 101, pp. 647-659, 2016. doi:10.1016/j.renene.2016.09.026

[9] C.Valero, M. Egusquiza, E. Egusquiza, A. Presas, D. Valentin, and M. Bossio, "Extension of operating range in pump-turbines. influence of head and load," Energies, vol. 10, pp. 2178, 2017. doi:10.3390/en10122178

[10] A. H. Slocum, M. N. Haji, A. Z. Trimble, M. Ferrara, S. J. Ghaemsaidi, "Integrated pumped hydro reverse osmosis systems," Sustainable Energy Technologies and Assessments, vol. 18, pp. 80-99, 2016. doi:10.1016/j.seta.2016.09.003

[11] M. Pérez-Sánchez, M. Simão, P. A. López-Jiménez, and H. M. Ramos, "CFD analyses and experiments in a PAT modeling: Pressure variation and system efficiency," Fluids , vol. 2, pp. 51, 2017. doi:10.3390/fluids2040051

[12] D. Buono, E. Frosina, A. Mazzone, U. Cesaro, A. Senatore, "Study of a Pump as Turbine for a hydraulic urban network using a tridimensional CFD modeling methodology," ATI 2015 - 70th Conference of the ATI Engineering Association, Energy Procedia 82, pp. 201 – 208, 2015. doi: 10.1016/j.egypro.2015.12.020

[13] F. X. Shi, J. H. Yang, and X. H. Wang. "Analysis on characteristic of pressure fluctuation in hydraulic turbine with guide vane," International Journal of Fluid Machinery and Systems, vol. 9, pp. 1882-9554, 2016. doi:10.5293/IJFMS.2016.9.3.237

[14] M. Venturini, S. Alvisi, S.Simani, and L. Manservigi. "Energy production by means of pumps as turbines in water distribution networks," Energies, vol. 10, pp. 1666, 2017. doi:10.3390/en10101666

[15] M. Sinagra, V. Sammartano, G. Morreale, and T. Tucciarelli. "A new device for pressure control and energy recovery in water distribution networks," Water, vol. 9, pp. 309, 2017. doi:10.3390/w9050309

[16] M. Kramer, K. Terheiden, and S. Wieprecht. "Pumps as turbines for efficient energy recovery in water supply networks," Renewable Energy, vol. 122, pp. 17-25, 2018. doi:10.1016/j.renene.2018.01.053

[17] M. C. Morani, A. Carravetta, G. Del Giudice, A. McNabola, and O. Fecarotta. "A comparison of energy recovery by PATs against direct variable speed pumping in water distribution networks," Fluids, vol.3, pp. 41, 2018. doi:10.3390/fluids3020041

[18] M. C. Chacón, J. A. R. Díaz, J. G. Morillo, and A. McNabola. "Pump-as-Turbine selection methodology for energy recovery in irrigation networks: Minimizing the payback period," Water, vol. 11, pp. 149, 2019. doi:10.3390/w11010149

[19] X. Wang, J. Yang, Z. Xia, Y. Hao, and X. Cheng. "Effect of velocity slip on head prediction for centrifugal pumps as turbines." Hindawi Publishing Corporation, Mathematical problems in engineering, 10 pages, Volume 2019. doi:10.1155/2019/5431047

[20] M. De Marchis, C.M. Fontanazza, G. Freni, A. Messineo, B. Milici, E. Napoli, V. Notaro, V. Puleo, and A. Scopa. "Energy recovery in water distribution networks. Implementation of pumps as turbine in a dynamic numerical model," 12th International Conference on Computing and Control for the Water Industry, CCWI2013, Procedia Engineering 70, pp. 439 – 448, 2013. doi: 10.1016/j.proeng.2014.02.049

[21] M. Rossi, M. Righetti, and M. Renzi. "Pump-as-Turbine for energy recovery applications: The case study of an aqueduct," 71st Conference of the Italian Thermal Machines Engineering Association, ATI2016, 14-16 September 2016, Turin, Italy, Energy Procedia 101, pp. 1207 – 1214, 2016. doi:10.1016/j.egypro.2016.11.163

[22] H.X. Shi, P. Chai, X.Z. Su, and R. Jaini. "Performance optimization of energy recovery device based on pat with guide vane." International-Journal-of-Simulation-Modelling. vol. 17, no. 3, pp. 472-484, 2018. doi:10.2507/IJSIMM17(3)443

[23] E. Frosina, D. Buono, and A. Senatore. "A performance prediction method for Pumps as Turbines (PAT) using a computational fluid dynamics (CFD) modeling approach," Energies, vol. 10, pp. 103, 2017. doi:10.3390/en10010103

[24] S. Yang, S. Derakhshan, and F. Kong. "Theoretical, numerical and experimental prediction of pump as turbine performance," Elsevier, Renewable Energy, vol. 48, pp. 507-513, 2012. doi:10.1016/j.renene.2012.06.002

[25] S. Yang, C. Wang, K. Chen, and X. Yuan. "Research on blade thickness influencing Pump as Turbine." Hindawi Publishing Corporation, Advances in Mechanical Engineering, 8 pages, Volume 2014. doi:10.1155/2014/190530

[26] S. Barbarelli, M. Amelio, G. Florio, and N.M. Scornaienchi. "Procedure selecting pumps running as turbines in micro hydro plants," 72nd Conference of the Italian Thermal Machines Engineering Association, ATI2017, 6-8

September 2017, Lecce, Italy, Energy Procedia, 126, pp. 549-556, 2017.

[27] S. C. Miao, J. Yang, F. Shi, X. Wang, and G. Shi. "Research on energy conversion characteristic of pump as turbine," Advances in Mechanical Engineering, vol. 10, pp. 1-10, February 2018. doi:10.1177/1687814018770836

[28] M. Venturini, S. Alvisi, S. Simani, and L. Manservigi "Comparison of different approaches to predict the performance of pumps as turbines (PATs)," Energies, vol. 11, pp. 1016, 2018. doi:10.3390/en11041016

[29] F. X. Shi, J.H. Yang, and X. Hui Wang. "Analysis on the effect of variable guide vane numbers on the performance of pump as turbine". Advances in Mechanical Engineering, vol. 10, pp. 1-9, 2018. doi:10.1177/1687814018780796

[30] S. Miao, J. Yang, G. Shi, and T. Wang. "Blade profile optimization of pump as turbine," Advances in Mechanical Engineering, vol. 7, pp. 1-9, 2015. doi:10.1177/1687814015605748

[31] Y. Sun, Z. Zuo, S. Liu, J. Liu, and Y. Wu. "Distribution of pressure fluctuations in a prototype pump turbine at pump mode," Hindawi Publishing Corporation, Advances in Mechanical Engineering, 10 pages, Volume 2014. doi:10.1155/2014/923937

[32] A. Arulmurugu, and P. V.Pandian. "Numerical investigation of centrifugal pump as turbine," Advances and Applications in Fluid Mechanics, vol. 17, pp. 147-163, 2015. doi:10.17654/AAFMApr2015_147_163

[33] W.C. Schleicher, and A. Oztekin. "Hydraulic design and optimization of a modular pump turbine runner". Energy Conversion and Management. vol. 93, pp. 388–398, 2015. doi.org/10.1016/j.enconman.2015.01.037.

[34] D. Li, Y. Sun, Z. Zuo, S. Liu, H. Wang, and Z. Li. "Analysis of pressure fluctuations in a prototype pump-turbine with different numbers of runner blades in turbine mode," Energies, vol. 11, pp. 1474, 2018. doi:10.3390/en11061474

[35] S. Fengxia, Y. Junhu, M. Senchun, and W. Xiaohui. "Investigation on the power loss and radial force characteristics of pump as turbine under gas–liquid two-phase condition," Advances in Mechanical Engineering, vol. 11, pp. 1-10, 2019. doi:10.1177/1687814019843732

[36] R. T. Knapp, Pasadena, Palif. "Complete characteristics of centrifugal pumps and their use in the prediction of transient behavior." Transactions of the American Society of Mechanical Engineers, pp. 683-689, 1937.

[37] J. Fernandez, E. Blanco, J. Parrondo, M. T. Stickland, and T. J. Scanlon. "Performance of a centrifugal pump running in inverse mode." Journal of power and energy. vol. 4, pp. 265-271, 2004. doi:10.1243/0957650041200632

[38] A. Carravetta, O. Fecarotta, R. Martino, and L. Antipodi. "PAT efficiency variation with design parameters," 12th International Conference on Computing and Control for the Water Industry, CCWI2013, Procedia Engineering 70, pp. 285 – 291, 2014. doi:10.1016/j.proeng.2014.02.032

[39] N. Raman, I. Hussein, K. Palanisamy, and B. Foo. "An experimental investigation of pump as turbine for micro hydro application," IOP Conference Series: Earth and Environmental Science, 16, 012064. 2013. doi:10.1088/1755-1315/16/1/012064

[40] S. Derakhshan, B. Mohammadi, and A. Nourbakhsh. "Efficiency improvement of centrifugal reverse pumps," Journal of Fluids Engineering, Vol. 131 / 021103-1, 2009. doi:10.1115/1.3059700

[41] G. Cavazzini, G. Pavesi, A. Santolin, G. Ardizzon, and R. Lorenzi. "Using splitter blades to improve suction performance of centrifugal impeller pumps," Journal of Power and Energy, vol. 229(3), pp. 309–323, 2015. doi:10.1177/0957650914563364

[42] Y. Sun-Sheng, K. Fan-Yu, F. Jian-Hui, and X. Ling. "Numerical research on effects of splitter blades to the influence of pump as turbine," Hindawi Publishing Corporation, International

Journal of Rotating Machinery, 9 pages, Volume 2012. doi:10.1155/2012/123093

[43] K. Jin-Woo , S. Jun-Won , C. Young-Seok , L. Kyoung-Yong , K. Joon-Hyung , T. Kanemoto, and K. Jin-Hyuk. “Simultaneous efficiency improvement of pump and turbine modes for a counter-rotating type pump-turbine.” Advances in Mechanical Engineering, vol. 8, pp. 1-14, 2016. doi:10.1177/1687814016676680

[44] P. Singh, and F. Nestmann. “Internal hydraulic analysis of impeller rounding in centrifugal pumps as turbines,” Elsevier, Experimental Thermal and Fluid Science, vol. 35, pp. 121-134, 2010. doi: 10.1016/j.expthermflusci.2010.08.013

Journal of Renewable Energy and Sustainable Development (RESD) Volume 5, Issue 2, December 2019 - ISSN 2356-8569
http://dx.doi.org/10.21622/RESD.2019.05.2.080

Natural Gas Pre-feasibility Study for Future LNG Importing Terminal Project in MOROCCO

[1] Firdaous EL GHAZI, [2] Moulay Brahim SEDRA, [3] Mahmoud AKDI
[1] Simolab, Ibn Tofail University, Kenitra, Morocco,
[2] FSTE, UMI Moulay Ismail University of Meknes, Morocco,
[3] Simolab, Ibn Tofail University, Kenitra, Morocco,
[1]elghazi.firdaous@gmail.com, [2] mysedra@yahoo.fr, [3] makerase@gmail.com

***Abstract* -** In recent years, energy debates are increasingly focused on the transition of more ecological energy sources, therefore, Morocco is projecting to invest in its first Liquified Natural Gas (LNG) importing and storage capacity by 2030. This article comes to establish a pre-feasibility study for the future importation terminal and the objective is to develop a scientific approach to investigate the financial viability of such a project. The main challenge poses on the data estimation methodology and the relevance of the assumptions. Besides, the level of uncertainty depends on the stability of the LNG international market.

The profitability of an investment is generally the most important criterion for the decision-making. Even if the combined ecological and industrial benefits of natural gas can sometimes provide enough motivation to invest, a long-term profitability study must be systematically pursued to evaluate the economic impact of such an investment decision.

After highlighting the multiple benefits of natural gas, the first step is setting up the financial model to be adopted, which is in this case the net present value (NPV) and the Discounted Payback. Therefore, operating and financial assumptions are made based on the benchmark with other similar projects. The pre-feasibility study will help to measure the LNG terminal capacity to generate revenue.

***Keywords* -** CAPEX, Cash Flow, Discounted Payback, GNL, Net Present Value, OPEX, Pre-Feasibility, Profitability..

I. INTRODUCTION

Global warming is a phenomenon known and recognized by scientists such as climate change and its adverse effects on the environment [1]. The history of energy between massive pollutions, nuclear disasters, energy resources scarcity and global environmental issues indicates the limitation of the current energy system and calls for a gradual shift towards a sustainable energy mix.

The global energetic context makes LNG an attractive alternative for electric and industrial generating units that currently run on other polluting, more expensive, and less suitable fuels. As a result, Morocco has set itself the goal of building an LNG import and storage terminal at Jorf Lasfar by 2030. In tune with developing a terminal site location and an optimum routing alternative for pipelines [2], this article comes as a follow up to conduct a pre-feasibility study for the future LNG importation terminal.

The reorientation of energy to LNG is a considerable step towards this objective. It is a source of clean energy that translates a strong commitment to:

- Replace the use of coal and harmful fuels in electricity production.
- Prepare a favorable economy that can be combined with renewable sources, particularly solar.
- Contribute to the development of energy efficiency.

Some countries, particularly Morocco, do not dispose of natural gas in their soil. In this case, their commitment is illustrated by an investment decision on LNG importing terminal. In the current economic environment, this decision is a decisive step that guides the national strategy.

II. CHOICE OF NATURAL GAS

The development of natural gas is driven not only by its availability as a resource, but also by its preference by consumers. Indeed, natural gas has several advantages and combines reliability, availability, cleanliness and safety as compared to nuclear energy.

A. Ecological Benefits

Compared to other fossil fuels, natural gas is considered by excellence the cleanest source of energy; its emissions of sulfur dioxide (SO2), carbon dioxide (CO2) and nitrous oxide are low compared to coal or oil [3]. In fact, a recent Greenpeace study, published in August 2019 and based on data from NASA [4], warns Morocco against the risks of air pollution due to the use of coal.

Fig .1 Nasa capture of SO2 hot spot, showcasing Morocco, 2019 [4]

The environmental qualities of natural gas largely justify the growth of its demand. With its high hydrogen content, its combustion is considered perfect and does not produce heavy unburnt.

B. Industrial Benefits

Natural gas continues to attract electric power plants and industrials because of its simple hydrocarbon composition (mainly methane) [5] whose use offers several advantages:

- Pure and perfect combustion: immediate and total flammability.
- Quality and precision of the flame: possibility of reaching very high combustion temperatures.
- Cleanliness: no emission of heavy polluting particles.
- Low maintenance: natural gas is not corrosive, it does not damage pipelines.
- Safety: restricted range of flammability.

C. Economic Benefits

The discovery and exploitation of natural gas is relatively newer than many other types of energy, hence its technology is naturally subject to several research development and technical progress. The entire chain of LNG, from exploration and drilling to end use, continues to gain efficiency and effectiveness.

The Moroccan global context makes LNG an attractive alternative for sectors currently running on other fossil fuels [6]. The LNG price competitiveness and the increasing number of stakeholders are only pulling its operating costs down, making it more and more attractive.

III. FINANCIAL AND PROFITABILITY CRITERIA

The investment decision is one of the strategic and irreversible decisions that engage resources in the long term. To evaluate the profitability of an investment and decide whether it should be retained, several methods can be used such as the Net Present Value (NPV) and the Payback method. These indicators rely on the estimated cash flows generated in a future environment.

The application of these financial techniques to evaluate the profitability of an investment is limited by the difficulty of modeling an economic reality of a distant and random market into a financial equation. Admittedly, the financial model of NPV is the most appropriate approach to decision making.

A. Net Present Value

In order to know if a given project is financially acceptable, the decision criterion considered is the NPV. Like any investment, the construction of an LNG terminal requires an investment period, an operating period, and a projected profitability that corresponds to the cash flows generated during the operating period. Thus, it is essential to estimate the following elements:

- Capital required for investment: The amount of funds necessary to conduct the project.
- The lifetime of the project: The operational period of the project or its useful life.
- The discount rate: The anticipated return of profit for a project which presents a similar risk, also called the cost of the invested capital.

- The annual cash flows: The remaining profit after revaluating the project's revenues and expenses.

The NPV is the difference between the investment and the annual project discounted cash flows. The discount rate corresponds to the required minimum rate of profit. A positive NPV indicates that the project is profitable, which means that the cash flows generated make it possible to reimburse the initial investments and generate added value

$$NPV = -I_0 + \sum_{i=1}^{n} \frac{CFi}{(1+t)^i} \quad (1)$$

With:
- i: a year in the project lifetime.
- I0: initial investment.
- CFi: cash flow generated during the operating year i.
- n: project lifetime.
- t: discount rate.

The discount rate is the cost of capital given its composition and the risk of the investment, assuming a discount rate of 9% [7].

B. Discounted Payback

To deepen the analysis, the evolution of the project payback is calculated according to the annual cash flow performed.

The payback is the time needed to recover the amount of the investment. This criterion allows to focus on projects quickly amortized, it is defined as the time required to recover the initial investment through cash inflows. This duration corresponds to the value of n for NPV = 0.

IV. MODEL DESCRIPTION AND ASSUMPTIONS

The investment required to carry out an industrial project of such a large size occupies an important place in the strategic launch decision. The profitability of an investment is completely determined when these two elements are known or at least can be accurately estimated: The amount of the investment also called Capital Expenditures (CAPEX) and the Operating Expenses (OPEX).

A. CAPEX Inventory

Several factors can influence the cost of building a terminal, feedback has shown that one of the most important factors is the quality of site environment, which can require some additional investments to limit and contain potential risks [8]. On the other hand, LNG storage tanks are generally the most expensive element of a storage terminal. They are also very often the most critical element because of the large surface area they claim, their visual impact that is often deemed unacceptable by the surrounding residents, and their potential risks if poorly managed.

1. LNG Storage Tanks

An LNG storage tank is particular and different from a hydrocarbon storage tank and has several challenges due to the specifications of the stored product, such as:

- The storage tank is intended to contain both vapor and liquid phases of natural gas.
- The storage tank must be insulated to minimize heat ingress.

The overall storage capacity of the site must meet the projected LNG consumption needs assessed by the Ministry of Energy as follows [9]:

Table 1 FIRST YEAR ANNUAL VOLUME OF IMPORTED NATURAL GAS [9].

	Year 1 (volume in k m3)
Volume gas to Power	3 500 000
Volume gas to Industry	1 500 000
Total Volume	5 000 000

According to the High Commission for Planning and considering an average growth of electricity consumption of 6% and an economic growth of 3% [10], the 20-year site import forecasts are as follows:

http://dx.doi.org/10.21622/RESD.2019.05.2.080

Table 2 LNG IMPORTING VOLUMES PROJECTIONS.

	Year 1	Year 2	Year 3	Year 4	Year 5	Year 6	Year 7	Year 8	Year 9	Year 10
Electricity growth %		5%	5%	5%	5%	5%	5%	5%	5%	5%
Volume gas to power (k m3)	3 500 000	3 675 000	3 858 750	4 051 688	4 254 272	4 466 985	4 690 335	4 924 851	5 171 094	5 429 649
Economic market growth %		3%	3%	3%	3%	3%	3%	3%	3%	3%
Volume gas to industry (k m3)	1 500 000	1 545 000	1 591 350	1 639 091	1 688 263	1 738 911	1 791 078	1 844 811	1 900 155	1 957 160
TOTAL Volume (k m3)	5 000 000	5 220 000	5 450 100	5 690 778	5 942 535	6 205 897	6 481 413	6 769 662	7 071 249	7 386 809

	Year 11	Year 12	Year 13	Year 14	Year 15	Year 16	Year 17	Year 18	Year 19	Year 20
Electricity growth %	5%	5%	5%	5%	5%	5%	5%	5%	5%	5%
Volume gas to power (k m3)	5 701 131	5 986 188	6 285 497	6 599 772	6 929 761	7 276 249	7 640 061	8 022 064	8 423 167	8 844 326
Economic market growth %	3%	3%	3%	3%	3%	3%	3%	3%	3%	3%
Volume gas to industry (k m3)	2 015 875	2 076 351	2 138 641	2 202 801	2 268 885	2 336 951	2 407 060	2 479 271	2 553 650	2 630 259
TOTAL Volume (k m3)	7 717 006	8 062 539	8 424 138	8 802 573	9 198 645	9 613 200	10 047 121	10 501 336	10 976 817	11 474 585

Table 3 SUPPLY FREQUENCY PER YEAR.

	Year 1	Year 2	Year 3	Year 4	Year 5	Year 6	Year 7	Year 8	Year 9	Year 10
Liquid GNL volume (km3)	8 333	8 700	9 084	9 485	9 904	10 343	10 802	11 283	11 785	12 311
Supply frenquency per year	23	24	25	26	28	29	30	31	33	34

	Year 11	Year 12	Year 13	Year 14	Year 15	Year 16	Year 17	Year 18	Year 19	Year 20
Liquid GNL volume (km3)	12 862	13 438	14 040	14 671	15 331	16 022	16 745	17 502	18 295	19 124
Supply frenquency per year	36	37	39	41	43	45	47	49	51	53

The sizing of the storage must allow the reception of the projected volumes and shall also guarantee flexibility in the case of a significant increase of the volumes. Natural gas is imported in the liquid phase and occupies 1/600 of its volume [11]. Thus, storage must be correctly sized to meet current and future forecast needs.

Given the many advantages of having multiple storage tanks, the breakdown of the storage would be as follows:

Table 4 BREAKDOWN OF THE TOTAL STORAGE CAPACITY.

Tank Diameter (m)	80
Tank height (m)	12
One Tank Capacity (m3)	60 288
Global Capacity - 6 tanks (m3)	361 728

With useful capacity of the importation terminal estimated at 360 000 m³, the supply frequency starts first with 2 importations per month and reaches on the 20th year 4 importations per month. Thus, the possibility of extending the storage remains possible. This storage capacity allows a good flexibility in cargos importation, two or three storage tanks can be used as principal linking distribution sources with the regasification process and the natural gas pipelines.

Using an average density of LNG of 445 kg / m³ and assuming $274/ton as the average world costs [12] for storage tanks, the CAPEX is:

Table 5 STORAGE CAPEX ESTIMATION.

Capacity in m3	Density in kg / m³	Capacity in ton	Average cost \$/t	CAPEX in \$
360 000	445	808 989	274	221 662 921

2. LNG Storage Tanks

The cost of the pipeline, on the other hand, can weigh heavily in the project investment amount. Its

cost depends on several parameters of which are mainly the type, the diameter and the length of the pipeline, the cost of the steel, the nature of the environment and the ground quality of its crossing. Assuming that the location of the importation terminal is in Jorf Lasfar and given the optimum pipeline routing, distance is calculated in the article “Study of site location and pipeline routing for future natural gas importing terminal project in Morocco” [2]. The shortest distance from Jorf Lasfar linking all consumption points including the furthest power station is 490 km.

Given that the investment reference announced for 5660 km of the Nigeria - Morocco pipeline project is estimated at 20 to 50 billion dollars [13] and considering the same pipeline characteristics for 490 km portion of the proposed routing, the pipeline investment can be roughly estimated at 1,8 to 4,5 billion dollars.

In order to estimate pipeline cost more accurately, several methods exist. The first is to launch a consultation procedure through a business consultation file; this approach makes it possible to acquire prices closest to the reality of the local market. Nevertheless, this approach is time consuming and is only applied at advanced stages of the project. On the other hand, a scientific formula developed by experts in this field can lead to a reliable estimation of the costs. It is a method developed by Menon, E._Shashi [14]:

Eq (2) pipeline $material\ cost$ (\$)

$$= 0{,}02463 \times (D - T) \times L \times T \times (cpt)$$

With:
L: Length of the pipe, km
D: Outside diameter of the pipe, mm
T: Thickness of the pipe wall
Cpt: Pipe cost, \$ / ton

Considering the American petroleum standard (API Spec 5L, ISO 3183), based on the united metallurgical company and the pipeline safety trust, the type of steel commonly used in natural gas pipeline construction, [15], the corresponding characteristic is:

L = 490 km
D = 40 ‘’
T = 9,5 mm - 236 Kg/ml
Cpt = 800 \$ / ton

Applying the formula, the estimated Capex for pipeline is:

$$Pipe\ material\ cost\ (\$) = 0{,}02463 \times (D - T) \times L \times T \times (cpt) = 2\,211\,352\,728\ \$$$

Many other aspects must be added to the pipeline investment such as:

Pipeline external coating and wrapping [14] are estimated at 5\$ per foot, therefore:

Pipe coating and wrapping cost = 50 × 0,3048 × 490 000 = 7 467 600 \$

Compressor Station Costs [14]: as the gas travels in the pipeline from high pressure areas to low pressure areas, it would be necessity to provide compressor stations which increase the internal pressure at regular intervals along the pipeline. Using an installed cost of 2 000\$ per compressor station and given that there must a compressor station every 20 km, the:

Compressor Station Costs = 2000 × 25 = 50 000 \$

SCADA and Telecommunication Systems [14], which correspond to the necessary automation and remote monitoring of the pipeline. SCADA system costs include facilities for monitoring, operating and remote control of the pipeline from a central control center. They are estimated as a percentage of the total project cost from 2% to 5%.

Environmental and Permitting [14]: due to stricter environmental and regulatory requirements, this category includes elements such as environmental impact reports, environmental studies of sensitive areas such as industrial sites and habitat areas. Authorization costs would include pipeline construction permits such as crossings of roads and railways. Costs related to the environment and authorizations can range between 10% and 15% of total project costs.

Other Project Costs [14] can cover unforeseen circumstances and design changes, including small diversions to bypass sensitive areas and modifications of facilities not originally planned at the beginning of the project. These costs can represent between 15% and 20% of the total cost of the project.

Table 6 PIPELINE COST ESTIMATION BREAKDOWN.

Pipe material	$2 211 352 728	
Coating and wrapping	$7 467 600	
	Min	Max
SCADA and Telecommunication (2% to 5% of total cost)	$60 789 598	$184 901 694
Environmental and Permitting (10% to 15% of total cost)	$303 947 990	$554 705 082
Other Project Costs (15% to 20% of total cost)	$455 921 985	$739 606 776
TOTAL Pipeline cost ($)	$3 039 479 902	$3 698 033 881

Thus, the global estimated pipeline cost is between 3 billion and 3,6 billion $.

It is important to record that the pipeline CAPEX is estimated to extend all CAPEX aspects but cannot be part of the profitability study itself. In fact, the scope of financial study is restricted in this article to the LNG importation terminal.

B. CAPEX Inventory

CAPEX estimation is a very important step as every site is specific in terms of capital cost. In general, considering the scope of the terminal alone, the storage tank represents the most important investment after the applicable maritime and process environment such as pump out and vaporizing process.

Based on the cost allocation for some similar LNG terminals conducted in a similar environment [16], the total CAPEX of the terminal is:

Table 7 CAPEX DISTRIBUTION OF THE IMPORTING TERMINAL.

	Cost Distribution	CAPEX in $
Jetty, topwork, trestle	10%	108 679 393
LNG storage	21%	221 662 921
Vaporizing, boil-off handling, pump out	39%	418 577 070
Utilities, offsites, fire and safety	19%	199 066 216
Allowance for land	3%	27 976 874
Owner's project management team	4%	43 041 344
Allowance for port and break water	5%	57 029 781
TOTAL CAPEX ($)	100%	1 076 033 599

Regasification itself represents 39% of the total cost of the project. The port equipment and LNG tanks are taking the large portion of the investments, with very large disparities related to site conditions.

Excluding the pipeline, the total CAPEX of the LNG importing terminal is estimated at 1 076 033,5 K$.

C. Operating Expenses

The specificity of the LNG market makes it difficult to estimate the operating expenses. The quantity imported depends on the national future consumption as the purchase prices and sales are very volatile. However, their trend is unpredictable and depends on several variables: currency rate, geopolitical stability, purchase contract or spot purchase, ocean freight, supplier countries, price indexation, etc.

The operation costs of an importation terminal are generally made up of the following items:

- Personnel cost and salaries: it is important to provide an organizational chart, with the estimated human resources and shifts. The wages are in general subject to variation depending on regions.
- Maintenance cost including corrective and preventive maintenance.
- Supply reception costs dedicated to LNG harbor and cargoes reception.
- Operating energy consumption.

Based on the OPEX data for some similar LNG terminals [16], the first year OPEX is estimated at 2,5% of the project CAPEX, the statistical distribution is then applied to recover the OPEX items:

http://dx.doi.org/10.21622/RESD.2019.05.2.080

Table 8 LNG TERMINAL OPEX DISTRIBUTION

	Cost Distribution	OPEX in $
Personnel salaries and/or wages	22%	6 033 833
Plant maintenance	26%	7 039 472
Marine Operations maintenance	37%	10 056 389
Energy Consumption	14%	3 771 146
TOTAL first year OPEX (2,5% of CAPEX)	100%	26 900 840

Once the CAPEX and OPEX are estimated, the profitability study can be perused.

V. PROFITABILITY OF THE LNG PROJECT

It is nearly impossible to speculate on the evolution of natural gas prices; therefore, a pricing reference is necessary to simulate the production and distribution margin. Considering the fluctuation in natural gas prices and according to the national LNG law project, Gas pricing will be regulated [9]. The prices hypothesis are based on the study on LNG prices of the Belgian market, published in 2018 [17], the Belgium market has many similarities with the Med Europe quotation market, therefore, the main hypothesis is as follows:

- Natural gas calorific power = 10,83 Kw/kg [18]
- Average import price = 14 €/MWh [17]
- Resale to power plants = 17 €/MWh [17]
- Resale price to industrial consumers = 18,9 €/MWh [17]
- Exchange rate 1 € = 1,1 $

A profitability analysis is carried out for the project considering all these factors during a 20 years lifetime. This life expectancy does not reflect the life of LNG terminal, but it is an economic life that can be used to evaluate the profitability of the project in the short/medium term. The longer the considered lifetime is, the more uncertain data are collected.

The financial calculation makes it possible to express the benefits of LNG terminal in monetary terms (profits) by comparing the revenues with the expenses while considering the monetary value of the time (by means of a discount rate).

Therefore:

The net present value (NPV) = $-I_0 + \sum_{i=1}^{n} \frac{CFi}{(1+t)^i}$

NPV = -176 563 k$ < 0

The project is financially not profitable.

Other financial indicators can be calculated to help us interpret profitability such as Profitability Index (PI) and Internal Rate of Return (IRR).

The profitability index is:

$$\frac{Future\ Cash\ Flows}{Initial\ Investment} = 1{,}29$$

The internal rate of return is the discount rate that makes the net present value (NPV) equal to zero.

$$NPV = -I_0 + \sum_{i=1}^{n} \frac{CFi}{(1+IRR)^i} = 0$$

Therefore, IRR= 7%

The discounted payback period is estimated at 12 year of operation, given a 9% discount rate.

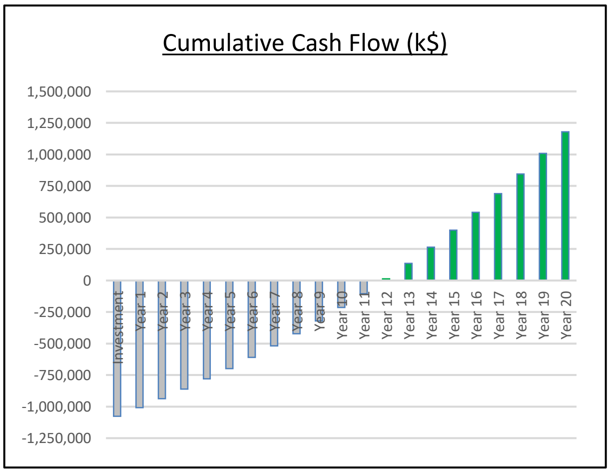

Fig .2 LNG terminal cash flow and discounted payback.

A 12-year payback means that the cash flows generated by LNG terminal is starting to recover the original investment from the 12th year of operation. It is important to point out that the cost of the distribution pipeline is not included, given the fact that the original pipeline is coming from Nigeria through many other countries, who can be participating in financing the pipeline. [2]

Table 9 LNG TERMINAL PROFITABILITY.

	Investment	Year 1	Year 2	Year 3	Year 4	Year 5	Year 6	Year 7	Year 8	Year 9	Year 10
TOTAL CAPEX (k$)	-1 076 034										
Gas to power volume (km3)		3 500 000	3 675 000	3 858 750	4 051 688	4 254 272	4 466 985	4 690 335	4 924 851	5 171 094	5 429 649
Gas to industry volume (Km3		1 500 000	1 545 000	1 591 350	1 639 091	1 688 263	1 738 911	1 791 078	1 844 811	1 900 155	1 957 160
TOTAL gas volume (Km3)		5 000 000	5 220 000	5 450 100	5 690 778	5 942 535	6 205 897	6 481 413	6 769 662	7 071 249	7 386 809
Operating and distribution margin (k$)											
Resale to power plants (k$)		315 426	331 198	347 758	365 146	383 403	402 573	422 702	443 837	466 029	489 330
Resale price to industrial consumers (k$)		151 087	155 619	160 288	165 096	170 049	175 151	180 405	185 817	191 392	197 134
TOTAL Operating income (k$)		466 513	486 817	508 045	530 242	553 452	577 724	603 107	629 654	657 421	686 464
Operating charges (k$)											
Average import price (k$)		-371 090	-387 418	-404 495	-422 358	-441 043	-460 589	-481 037	-502 431	-524 814	-548 234
OPEX k$ (2% inflation)		-26 901	-27 439	-27 988	-28 547	-29 118	-29 701	-30 295	-30 901	-31 519	-32 149
TOTAL Terminal charges (k$)		-397 991	-414 857	-432 483	-450 905	-470 161	-490 290	-511 332	-533 331	-556 333	-580 383
Net Cash Flow (k$)	-1 076 034	68 522	71 960	75 562	79 336	83 291	87 434	91 775	96 323	101 088	106 081
Cumulative Cash Flow (k$)	-1 076 034	-1 007 511	-935 551	-859 989	-780 652	-697 361	-609 927	-518 153	-421 830	-320 742	-214 661

	Year 11	Year 12	Year 13	Year 14	Year 15	Year 16	Year 17	Year 18	Year 19	Year 20
TOTAL CAPEX (k$)										
Gas to power volume (km3)	5 701 131	5 986 188	6 285 497	6 599 772	6 929 761	7 276 249	7 640 061	8 022 064	8 423 167	8 844 326
Gas to industry volume (Km3	2 015 875	2 076 351	2 138 641	2 202 801	2 268 885	2 336 951	2 407 060	2 479 271	2 553 650	2 630 259
TOTAL gas volume (Km3)	7 717 006	8 062 539	8 424 138	8 802 573	9 198 645	9 613 200	10 047 121	10 501 336	10 976 817	11 474 585
Operating and distribution margin (k$)										
Resale to power plants (k$)	513 796	539 486	566 461	594 784	624 523	655 749	688 536	722 963	759 111	797 067
Resale price to industrial consumers (k$)	203 048	209 139	215 413	221 876	228 532	235 388	242 450	249 723	257 215	264 931
TOTAL Operating income (k$)	716 844	748 626	781 874	816 659	853 055	891 137	930 986	972 686	1 016 326	1 061 998
Operating charges (k$)										
Average import price (k$)	-572 741	-598 385	-625 223	-653 309	-682 705	-713 472	-745 677	-779 388	-814 677	-851 621
OPEX k$ (2% inflation)	-32 792	-33 448	-34 117	-34 799	-35 495	-36 205	-36 929	-37 668	-38 421	-39 189
TOTAL Terminal charges (k$)	-605 533	-631 833	-659 339	-688 108	-718 200	-749 677	-782 606	-817 056	-853 098	-890 810
Net Cash Flow (k$)	111 312	116 792	122 535	128 551	134 855	141 460	148 380	155 631	163 228	171 188
Cumulative Cash Flow (k$)	-103 350	13 443	135 977	264 528	399 383	540 843	689 223	844 853	1 008 081	1 179 270

VI. CONCLUSIONS

An investment in a national LNG importing terminal is an important decision requiring a huge investment. After assimilating at first the other non-financial benefits of natural gas, a financial model description and LNG market hypothesis were considered and exposed in order to provide a reliable pre-feasibility study regarding the available data now for the Moroccan market.

At this stage of the project, accuracy of these estimates is believed to be +/-40%. The conducted financial study shows that the project is not profitable within 20 years lifetime, but has estimated payback of 12 years of operation, excluding the pipeline investment. The NPV is negative and the IRR (7%) is inferior to the discount rate (9%), which reflects that, mathematically, this project will not be profitable enough even after 20 years of operating.

These results justify the fact that the profitability of this kind of investment requires government encouragement through subsidies and tax reduction. The environmental qualities of natural gas largely justify the conduction of this project. With its high hydrogen content, gas combustion is considered perfect and does not produce heavy unburnt harmful particles for environment or health. Given the tax incentives and government conventions planned in Morocco to encourage the use of natural gas, the profitability of this investment is guaranteed on a long term.

The profitability is generally the most important criterion for the decision-maker, who can also base his judgment on other non-quantitative criteria of an economic or strategic nature, however, investment in ecological energy is a strategic decision that cannot be reduced to a calculation of mathematical expectations. Certainly, financial analysis is of paramount importance in the decision-making process, but some non-financial and non-quantifiable criteria must be taken into account.

REFERENCES

[1] R. Laplante, F. L'Italien, N. Mousseau, and S. Labranche, "How to get out from fossil fuel". 2nd International Summit Of Research Cooperatives In Community Development, Energy Transition, UNIVERSITY OF QUEBEC, available on: http://normandmousseau.com/publications/159.pdf [2015]

[2] M. Akdi, F.El Ghazi, and M.B.Sedra, "Study of site location and pipeline routing for future natural gas importing terminal project in Morocco", Journal of Renewable Energy and Sustainable Development (RESD), vol. 5, Issue 1, June 2019 - ISSN 2356-8569 [2019].

[3] G. Bern, Bloomberg Financial series, Investing in Energy, "a primer on the economics of the energy industry", available on: https://www.wiley.com/en-us/Investing+in+Energy%3A+A+Primer+on+the+Economics+of+the+Energy+Industry-p-9781576603758 [2011]

[4] S. Dahiya and L. Myllyvirta, "Global SO2 emission hotspot database, Ranking of the world's worst sources of SO2 pollution", Greenpeace Environment Trust, Aug [2019]

[5] D. Flowers, S. Aceves, C. K. Westbrook, J. R. Smith, and R. Dibble, Detailed Chemical Simulation of Natural Gas Combustion: Gas Composition Effects and Investigation of Control Strategies. Place of publication: publisher [2000]

[6] A.Amara, "Roadmap of the national development plan for liquefied natural gas", Ministry of Energy, Mines, Water and Environment, p. 11, available on: https://fr.scribd.com/doc/250255788/Plan-National-Marocain-de-Developpement-Du-Gaz-Naturel-Liquefie-Gnl [2014].

[7] "Note on Value for Money", Handbook of good practices, Ministry of Economics and Finance, May [2018]. Available on: https://www.finances.gov.ma/Docs/depp/2018/Note%20sur%20la%20Value%20for%20Money%20VF%202016.pdf

[8] R. Tarakad, "LNG receiving and regasification terminals, an overview of design", Operation and Project Development Consideration, pp. 31--34, place of publication: publisher [2003]

[9] Law Project Relating to the Downstream Sector of Natural Gas in Morocco. N° 9417 Ministry of Energy, Mines, Water and Environment, [2017]

[10] "Prospective Morocco 2030", High Commissariat Planning, Kingdom of Morocco, [2019] https://cnd.hcp.ma/Conjoncture-du-08-au-12-Juillet-2019_a1440.html

[11] The International Group of Liquified Natural Importers, GIIGNL annual report [2019] available on: https://giignl.org/sites/default/files/PUBLIC_AREA/Publications/giignl_annual_report_2019-compressed.pdf

[12] "World LNG report", 27th World Gas Conference, p. 53 [2018]

[13] Benchmark of the Royal Institute of Strategic Studies [2018], available on: https://www.medias24.com/MAROC/ECONOMIE/ECONOMIE/188546-Gazoduc-Maroc-Nigeria-Voici-un-benchmark-de-l-Institut-royal-des-etudes-strategiques.html

[14] SYSTEK Technologies, Inc., USA, TRANSMISSION, PIPELINE: CALCULATIONS AND SIMULATIONS MANUAL, p. 489, [2015]

[15] JSC "United Metallurgical Company" and "Pipeline Basics & Specifics About Natural Gas

http://dx.doi.org/10.21622/RESD.2019.05.2.080

Pipelines" available on [2015] https://omksteel.com/upload/iblock/3f9/OMK%20large%20diameter%20pipes%20catalogue.pdf and http://pstrust.org/wp-content/uploads/2015/09/2015-PST-Briefing-Paper-02-NatGasBasics.pdf

[16] R. Tarakad, LNG Receiving and Regasification Terminals, an Overview of Design, Operation and Project Development Consideration, Houston Texas, p. 102, Zeus Corporation Corp, [2003]

[17] Belgium Commission for Regulating Electricity and Gas, "Study on prices on the Belgian Natural Gas Market in 2017, pp. 9-10, [2018]

[18] Pickbleu, "Comparative table lower caloric energy (PCI) of energies", [2017], available on https://www.picbleu.fr/page/tableau-comparatif-pouvoir-calorique-inferieur-pci-des-energies.

Journal of
Renewable Energy and Sustainable Development

RESD

Volume 5, Issue 2, December 2019 ISSN 2356-8569

ISSN 2356-8569

http://apc.aast.edu

مركز الأكاديمية للنشر
ACADEMY Publishing Center